International Geology Review
2011, iFirst article, 1–22

Taylor & Francis
Taylor & Francis Group

Chemical geodynamics of Western Anatolia

Ramananda Chakrabarti[a,b], Asish R. Basu[a]* and Arundhuti Ghatak[a]

[a]*Department of Earth and Environmental Sciences, University of Rochester, Rochester, NY 14627, USA;* [b]*Department of Earth and Planetary Sciences, Harvard University, Cambridge, MA 02138, USA*

We report major and trace element concentrations and Nd–Sr–Pb isotopic data of 10 post-collisional volcanic domains in Western Anatolia, a seismically active part of the Alpine–Himalayan belt in the Aegean extensional province. Our objective is to provide geochemical constraints for tectono-magmatic processes shaping the late Cenozoic geodynamic evolution of Western Anatolia.

Calc-alkaline volcanic rocks occurring to the north of the Izmir–Ankara–Erzincan suture zone show arc-like trace elements and isotopes and were formed by the melting of the metasomatized Neotethyan mantle-wedge; this process was facilitated by asthenospheric upwelling resulting from slab delamination. Calc-alkaline and alkaline volcanic rocks from within the Izmir–Ankara–Erzincan suture zone also show the imprint of subduction fluids in their major and trace elements, but their isotopic compositions indicate derivation from a metasomatized lithospheric mantle followed by assimilation of ancient crust. Volcanics along the N–S-oriented Kirka–Afyon–Isparta trend were derived from the lithospheric mantle that was metasomatized by fluids from the older subduction of the African plate. Golcuk–Isparta volcanic rocks show an asthenospheric imprint; the latter was a consequence of upwelling following a tear in the subducting African lithosphere. Shoshonitic Kula volcanic rocks show very high trace element concentrations, OIB mantle-like trace elements, and Nd–Sr–Pb isotopic signatures, and were formed by partial melting of the upwelling asthenospheric mantle; this event was synchronous with the Aegean extension and possibly also with slab window formation due to ruptures in the African plate.

Inherent in the above chemical geodynamic models are the high $\varepsilon_{Nd(0)}$ values (+6.4) of the end-member volcanic rocks, implying the presence of an asthenospheric source beneath Western Anatolia that is responsible for the currently observed high heat flow, low Pn wave velocities, high seismicity, and tectonic activity.

Keywords: Western Anatolian volcanic rocks; major and trace element concentrations; Nd–Sr–Pb isotopic data; subduction; extension

1. Introduction

The dynamic evolution of the Earth's continents is primarily controlled by subduction and collisional processes. Evidence of such subduction–collisional processes is found in rocks of various ages in global orogenic belts. The Alpine–Himalayan belt is a relatively modern example of such an orogenic belt, where continental collision is continuing by convergence of continental plates, followed by extension in parts of this orogen. The Western Anatolian region, the focus of this study, is one of the most seismically active regions of the Alpine–Himalayan orogenic belt. It had an earlier history of predominantly convergent tectonics but currently displays mostly extensional features.

Many orogenic belts are marked by post-collisional calc-alkaline and alkaline magmatism. Geochemical and petrogenetic studies of post-collisional magmatism can provide constraints on the inferred geodynamic processes responsible for the cessation of collision and onset of extensional collapse, as well as changes in magma source regions and associated processes. A transition from older calc-alkaline magmatism to younger intraplate alkaline magmatism has been reported from several post-collisional volcanic provinces such as the Western Mediterranean (Coulon et al. 2002), Papua New Guinea (Hegner and Smith 1992), Northwest Iran (Innocenti et al. 1982), New Mexico, southwest USA (Davis and Hawkesworth 1993), and Western Anatolia (Gulec 1991; Aldanmaz et al. 2000; Yilmaz et al. 2001; Altunkaynak and Genc 2008). This transition in magmatic compositions has been attributed to several factors including the cessation of subduction at previously convergent margins (Cole and Basu 1992) and post-collisional tensional tectonics (Venturelli et al. 1984). Subduction rollback and lithospheric delamination are also recognized as important geodynamic processes (Houseman et al. 1981), and the consequences of these processes should be reflected in changes in sources of magmas erupted during different phases of orogenic development. The possible roles of these processes in the geodynamic evolution of Western Anatolia have been discussed by several authors (Seyitoglu and Scott 1996; Aldanmaz et al. 2000; Koprubasi and Aldanmaz 2004; Dilek and Altunkaynak 2007).

*Corresponding author. Email: asish.basu@rochester.edu

ISSN: 0020-6814 print/1938-2839 online

DOI: 10.1080/00206814.2010.543787
http://www.informaworld.com

In this study, we report major and trace element concentrations as well as Nd–Sr–Pb isotopic data for 40 Cenozoic volcanic rock samples selected from 10 different post-collisional domains in Western Anatolia (Figure 1B). The majority of these volcanic domains have not been geochemically studied previously. In particular, Pb isotopic data for Western Anatolian volcanic rocks are sparse. This study complements the existing geochemical data from several other volcanic provinces in Western Anatolia. The purpose of our study is to provide a better understanding of the tectono-magmatic processes shaping the geodynamic evolution of Western Anatolia since the Cenozoic. Our geochemical and combined Nd–Sr–Pb isotopic data should allow an evaluation of the various competing tectonic processes, and the links between magmatism, lithosphere kinematics, and upper mantle flow in different parts of Western Anatolia. Our new analytical results, particularly the isotopic data for these volcanic rocks, have implications for an improved understanding of collision and subduction-related asthenospheric dynamics, and hence for developing tectonic models that would allow better characterization of the observed seismicity and volcanism within this densely populated area of the Mediterranean region in Western Anatolia.

2. Geological background

Neotectonic evolution of the eastern Mediterranean region (Bozkurt 2001) is believed to be controlled mainly by three geodynamics processes: collision of the Arabian plate with Eurasia along the Biltis–Pontides collisional belt since late the Oligocene–early Miocene (Faccenna et al. 2006), the resultant westward escape of the Anatolian block away from the Arabia–Eurasia collision zone along the North and East Anatolian fault systems (McKenzie 1972; Sengor et al. 1985; Taymaz et al. 1991), and subduction of the African plate beneath Eurasia along the Hellenic and Cyprean trenches since the early Miocene (∼26 Ma) (Jackson and McKenzie 1988a, 1988b; Meulenkamp et al. 1988) (Figure 1A and 1B).

Anatolia was part of Gondwanaland during the Permian (Sengor and Yilmaz 1981; Aldanmaz et al. 2000; Piper et al. 2002). Rifting of Gondwanaland during Late Triassic formed the Cimmerian continent and initiated the formation of the Neotethys. During Early Jurassic, rifting of Cimmeria resulted in the formation of the Anatolide–Tauride platform between two branches of the Neotethys (Sengor and Yilmaz 1981). Cimmeria–Eurasia collision in the Middle Jurassic led to the closure of Palaeotethys followed by northerly subduction of the Neotethyan plate (Okay et al. 1998), forming the Pontide arc. This subduction led to the closure of Neotethys during Late Cretaceous to Palaeocene followed by collision of the Anatolide–Tauride platform with the Sakarya continent along the Izmir–Ankara–Erzican Suture Zone (IAESZ) (Okay et al. 1998; Candan et al. 2005) (Figure 1). The timing of this Alpine-style collision is not well constrained but is estimated to be around Palaeocene–mid-Eocene (Harris et al. 1994).

The Anatolian block is undergoing active internal deformation as Central Anatolia is moving westward relative to Eurasia at a rate of ∼15 mm/year whereas Western Anatolia [west of the Isparta Angle (IA); Figure 1A and 1B] is moving southwest at ∼30 mm/year (Reilinger et al. 1997). Africa and Eurasia are converging at ∼10 mm/year, although the convergence rate across the Hellenic Trench is greater than 40 mm/year (McClusky and Balassanian 2000). Subduction rollback along the Hellenic Trench since ∼12 Ma (Meulenkamp et al. 1988) caused extension in the upper plate, resulting in the development of the Aegean extensional province, which is undergoing ∼N–S extension at 30–40 mm/year (Taymaz et al. 1991; Le Pichon et al. 1995; Oral et al. 1995). Structural studies of fault-bound Palaeogene–Neogene sedimentary basins and metamorphic core complexes in this region suggest that the extension is likely to have begun ∼25 Ma in parts of the southern Aegean due to orogenic collapse of an over-thickened crust created during the Palaeogene compressional regime (Seyitoglu and Scott 1992; Jolivet et al. 1994). However, it has been suggested that extension in western Turkey occurred in two stages separated by 5–7 Ma (Bozkurt 2003). The second Plio-Quaternary phase of N–S extension is related to the westward escape of the Anatolian block as mentioned above.

Western Anatolia has experienced extensive post-collisional volcanism since the late Eocene. The oldest volcanics are ∼37.3 million years old, whereas the youngest volcanics are 0.13 ± 0.05 million years old (Yilmaz 1990; Gulec 1991; Ercan et al. 1995; Richardson-Bunbury 1996; Savascin and Oyman 1998; Aldanmaz et al. 2000). These volcanics are hosted by a continental crust that was first thickened and subsequently thinned by orogenic processes (Aldanmaz et al. 2000; Dilek and Altunkaynak 2007). Granitoid plutons (54–34 million years old), occurring in an E–W-trending zone between the Sea of Marmara and the IAESZ, were also emplaced in a post-collisional setting (Harris et al. 1994; Okay and Satir 2000; Koprubasi and Aldanmaz 2004; Altunkaynak 2007; Dilek and Altunkaynak 2007). Cenozoic volcanism in Western Anatolia has evolved from calc-alkaline character with mostly mafic to intermediate and acidic products to dominantly mafic, alkaline compositions. This compositional variation possibly reflects a change in the tectonic regime from N–S compression to extension (Yilmaz 1989; Savascin 1990; Yilmaz 1990; Altunkaynak and Genc 2008). The subduction of the African lithosphere beneath Eurasia along the Hellenic Trench dates back only to early Miocene (∼26 Ma) (Meulenkamp et al. 1988). Hence, the initial calc-alkaline volcanism in Western Anatolia was post-collisional and not related to any active subduction

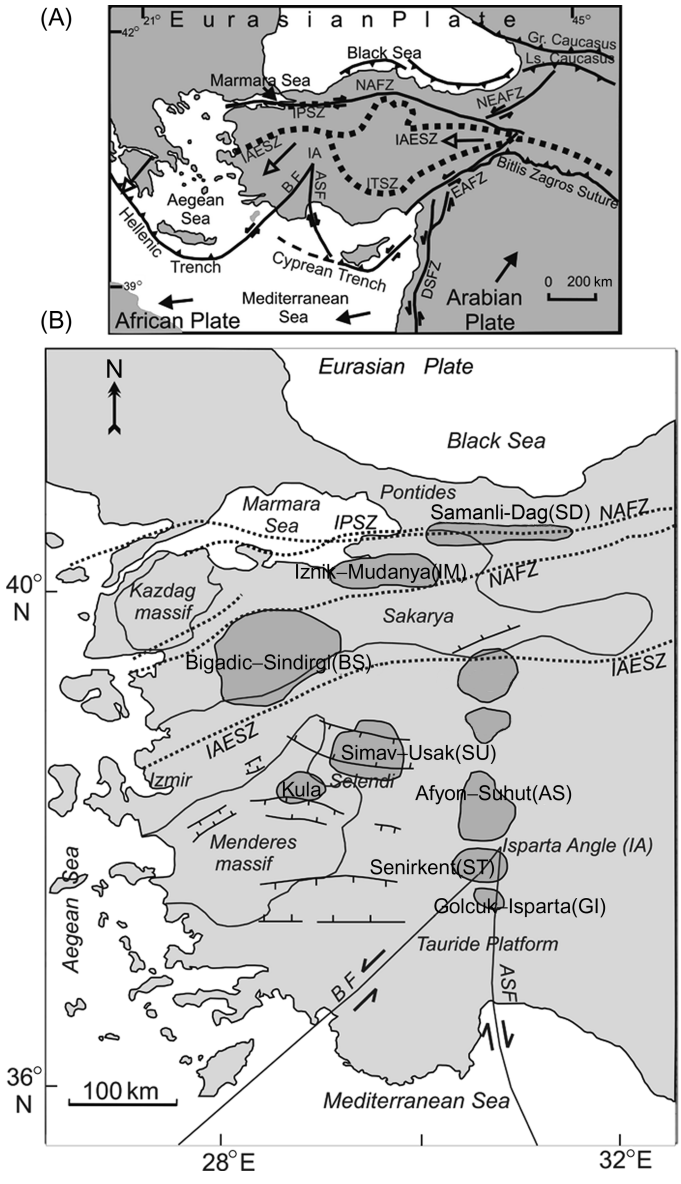

Figure 1. (A) A general map of the Mediterranean region including the Anatolian province showing the major tectonic features including the Northern Anatolian Fault Zone (NAFZ), Eastern Anatolian Fault Zone (EAFZ), Intra-Pontide Suture Zone (IPSZ), Izmir–Ankara–Erzincan Suture Zone (IAESZ), Isparta Angle (IA), Burdur Fault (BF), and the Alsaher–Simav Fault (ASF). The arrows indicate the movement directions of the different tectonic plates. Western Anatolia is located to the east of the Aegean Sea and to the west of the IA. (B) Distribution of the 10 volcanic domains (outlined grey regions) of this study in Western Anatolia. Also shown are the basement sequences – the Sakarya Continent, the Kazdag and Menderes massifs as well as the Intra-Pontide Suture Zone (IPSZ), the Northern Anatolian Fault Zone (NAFZ), the Izmir–Ankara–Erzincan Suture Zone (IAESZ), the Isparta Angle (IA), the sedimentary Tauride platform, the Burdur Fault (BF), the Alsaher–Simav Fault (ASF), and some prominent grabens.

at that time, but the influence of older subduction systems in modifying the magma source composition cannot be ruled out.

In this study, our investigation of the various Western Anatolian volcanic suites is expected to contribute to improving the present knowledge and understanding of the geological and plate dynamic background of Western Anatolia as discussed above.

3. Sample description and geochemical tracer results

Forty post-collisional volcanic rock samples, belonging to 10 different volcanic domains of Western Anatolia, were analysed in this study (Figure 1B) for major and trace element concentrations and Nd–Sr–Pb isotopes. Detailed analytical methods are given in Appendix 1. The wide variations in the geochemical and isotopic compositions of

these volcanics, as discussed below, are a result of complex tectonic processes in this region since the Cenozoic.

Major and trace element concentrations of these volcanics are shown in Table 1 and their Nd–Sr–Pb isotopic compositions are shown in Table 2. Nd–Sr–Pb isotopic ratios for these young volcanics are not age corrected (except for Kirka) because of the lack of available precise age data for the different volcanic domains (Appendix 1). More importantly, the samples of this study show overall low parent/daughter isotope ratios in the Sm/Nd, Rb/Sr, and U/Pb systems; also, considering the relatively young age of eruption, the measured isotopic ratios, in most cases, are assumed to be initial ratios. The Kirka sample is an exception that has an unusually high Rb/Sr ratio and hence its initial Sr isotopic composition at 21 Ma (Savascin 1990) is reported. U/Pb and Th/Pb ratios in these volcanic rocks show a wide range, possibly reflecting post-eruptive mobilization of fluid-mobile elements such as Pb and U. Their measured Pb isotopic compositions are therefore considered as initial.

As mentioned above, age estimates are not available for all the volcanic domains studied here. Hence, we have utilized the geochemical and isotopic compositions of these volcanics as determined in this study, their basement characteristics, available age estimates for some domains, and their spatial relation to major tectonic features to categorize them into broad groups as described below. The different basement rocks include (i) the Sakarya crystalline rocks (between Intra-Pontide Suture Zone and IAESZ) and the ophiolitic and accretionary-type mélange units of the Karakaya Complex to the north (Tekeli 1981; Altunkaynak 2007), (ii) ophiolites from the IAESZ, (iii) Jurassic carbonates around the IAESZ, (iv) Menderes metamorphic massif, (v) Palaeozoic–Mesozoic carbonates, and (vi) Triassic rift assemblages of the Taurides (Figure 1B).

The Samanli-Dag volcanics occur along the northern edge of the Sakarya Continent and within the northern branch of the North Anatolian Fault Zone (NAFZ), whereas the Iznik–Mudanya volcanics occur in an E–W-trending narrow zone within the Sakarya Continent. The composite continental block comprising the Sakarya Continent and Karakaya Complex is the basement for these volcanics for which there are no available radiometric ages. The Samanli and Iznik volcanics, located to the north of the IAESZ (Figure 1B), are calc-alkaline with low K_2O contents ranging from basalts and basaltic andesites to basaltic trachyandesites and andesites in the K_2O versus SiO_2 plot (Peccerillo and Taylor 1976) and the total alkali silica plot (Le Bas and Streckeisen 1991) (Figure 2A and 2B) with moderate MgO contents (1.71–4.15 wt.%) (Figure 2C). They show a light rare earth element (LREE) enriched and a flat heavy rare earth element (HREE) pattern (Figure 3A, chondrite normalized) and in primitive mantle-normalized trace element plots (Figure 3B) show higher concentrations of the large-ion lithophile elements (LILEs) compared with the high field strength elements (HFSEs), resulting in prominent Nb–Ta depletions. Other characteristic geochemical features include low chondrite-normalized La/Yb (Figure 4A), wide-ranging Ba/La (Figure 4B), relatively low Th/Yb and Ta/Tb (Figure 4C), as well as arc-like Ce/Pb (Miller et al. 1994) (Figure 4D). Samanli-Dag sample 04-WAV showing anomalously high K_2O (8.74 wt.%) but low Na_2O, more fractionated $La/Sm_{(\tilde{N})}$ and comparatively higher trace element concentrations, occurs as a dike. These volcanics show relatively radiogenic Nd isotopic compositions ($\varepsilon_{Nd(0)} = +0.9$ to $+6.4$) as well as radiogenic Sr (0.714190–0.706223) compared with the mantle array (Figure 5A) at low Rb/Sr (Figure 5B). Pb isotopic composition is relatively unradiogenic as shown in Figure 6 and Table 2.

The Bigadic–Sindirgi volcanics occupy a larger area immediately south of the southern branch of the NAFZ and include 21–15 million-year-old (Erkul et al. 2005) intermediate to acidic lavas and pyroclastic rocks. They occur within the IAESZ and their basement rocks are either ophiolites or carbonates. These rocks constitute an eastward extension of calc-alkaline volcanics in the Biga Peninsula previously described (Aldanmaz et al. 2000; Altunkaynak and Genc 2008) and are high-K calc-alkaline rocks with a compositional bimodality in major element (Figure 2) and Nd–Sr–Pb isotopic compositions as well as Rb/Sr ratios (Figure 5). However, their trace element concentration patterns are overall uniform with LREE enrichment and negative Nb–Ta anomaly (Figure 3). Positive anomalies of Pb, Sr, Zr, and Hf are observed in varying degrees (Figure 3) together with high Ba/La, Th/Yb, low Ce/Pb (Figure 4), and radiogenic Sr and Pb and unradiogenic Nd isotopes (Figures 5 and 6). One Bigadic sample (19-WAV) shows unusually fractionated LREE with anomalously high La ($\sim$800$\times$ chondrite).

Also hosted within the IAESZ ophiolites are the 11–6 million-year-old Seyitgazi volcanics that are basaltic trachyandesites and enriched in K_2O, with lower SiO_2 and higher MgO (Figure 2), in contrast to the subalkaline Bigadic volcanics. They show LREE enrichment although the LILE enrichment is not pronounced compared with the HFSEs (Figure 3B). Compared with the Bigadic lavas, the Seyitgazi volcanics also show considerably lower Ba/La (Figure 4B) and high Th/Yb (Figure 4C) but more radiogenic $^{206}Pb/^{204}Pb$ (Figure 6) as well as lower Rb/Sr (Figure 5B). In an Nd–Sr isotope plot (Figure 5A), these volcanics plot in the enriched quadrant, although with less radiogenic Sr and more radiogenic Nd compared with the Bigadic lavas.

The Kirka volcanics are located to the immediate south of the IAESZ. The Kirka sample is a rhyolite with no radiometric age data available, although it is estimated that these volcanics may be as old as 21–17 million years (Savascin and Oyman 1998). The Afyon–Suhut volcanics contain 14–8.7 Ma trachytic lavas and domes intercalated

Table 1. Selected major (wt.%) and trace element (μg/g) concentrations and elemental ratios of the studied Western Anatolian volcanic rocks.

	Samanli				Iznik			Bigadic										Golcuk			
Sample	1wav	3wav	4wav	5wav	7wav	8wav	9wav	10wav	12wav	13wav	14wav	15wav	16wav	17wav	18wav	19wav	20wav	40wav	41wav	42wav	44wav
SiO_2	51	51.5	48.5	48.2	55	60.3	51.2	57.2	64.8	58.3	58.1	57.5	58.7	66.9	67.9	66	65.8	53.7	52.4	53.5	52.4
Al_2O_3	18.5	18.3	16.3	17.7	17.6	15.3	19.1	17.1	15	16.8	17.7	17.4	16.9	16.3	16.3	15.5	16.7	16	15.5	16.6	15.9
Fe_2O_3	8.55	9.01	9.93	10.5	7.33	7.82	7.4	6.11	3.84	6.69	6.19	6.98	6.73	2.16	2.14	3.46	2.77	6.29	6.73	6.06	7.08
MnO	0.11	0.13	0.18	0.14	0.10	0.12	0.11	0.12	0.05	0.1	0.12	0.13	0.14	0.02	0.03	0.04	0.03	0.12	0.13	0.14	0.12
MgO	2.94	4.15	3.58	4.05	1.71	1.79	2.69	3.34	1.56	2.74	2.46	2.52	2.46	0.56	0.71	1.37	0.76	3.01	4.01	2.39	2.95
CaO	8.23	4.01	8.8	8.97	6.43	3.5	8.76	6.43	3.24	6.4	6.12	6.32	5.82	3.21	3.13	3.66	3.28	6.90	8.25	6.67	7.65
Na_2O	4.04	6.18	1.75	3.39	5.13	6.32	3.9	3.51	3.31	3.46	3.35	3.77	3.43	3.67	3.54	3.61	3.76	5.07	4.20	3.41	1.92
K_2O	0.58	0.44	8.74	0.34	1.43	0.38	0.53	2.52	3.49	2.14	2.41	2.34	2.38	3.25	3.2	3.27	3.89	5.28	5.24	6.44	4.16
TiO_2	0.72	1.08	1.64	1.53	0.66	0.85	1.18	0.65	0.55	0.64	0.71	0.82	0.73	0.53	0.5	0.5	0.58	0.77	0.72	0.84	1
P_2O_5	0.17	0.15	0.67	0.36	0.17	0.15	0.21	0.24	0.17	0.16	0.23	0.19	0.24	0.16	0.16	0.16	0.19	0.7	0.84	0.60	0.78
LOI	3.9	4.3	0.2	3.90	3.2	2.2	3.6	1.6	2.9	2.7	1.8	2.2	1.4	1.9	2	1.80	2.2	0.7	1.7	3.3	5.7
Rb	8.5	7.2	572	4.7	40.2	5.8	9.5	103	113	64	72	67	75	109	111	109	125	80	122	78	32.9
Sr	355	373	1813	297	733	345	328	570	344	539	827	476	607	378	366	347	334	5912	5958	6558	6717
Y	19.4	28.1	34.9	53	22.9	32.3	27.8	20.7	17.2	24.5	26.9	28.9	31.8	17.8	14	28.1	19.5	41.3	36	35.2	43.5
Zr	75	98	862	248	138	133	143	159	35.6	123	166	164	187	32	31.2	31.7	40.5	538	471	850	885
Nb	2.62	4.22	58	6.88	4.63	5.76	8.69	14	15.2	11.2	10.6	10.4	11.5	17	15.3	14.7	16.7	79	56	116	119
Ba	214	148	1551	133	332	148	121	955	900	973	1369	902	1658	921	1044	865	989	3455	3661	8437	4724
La	7.06	7.99	30.5	17.4	24.9	13.6	14.1	29.3	27.4	32.2	31.3	29.5	35.6	25.8	38.7	307	24.5	337	252	268	281
Ce	15.7	19.8	63	43.9	43.1	30.3	32.8	56	49	62	62	58	65	47.2	72	526	47.6	627	482	485	525
Pr	2.11	2.79	7.7	6.05	4.81	3.87	4.11	6.08	5.99	7.14	7.03	6.78	7.67	5.55	7.88	48.8	5.49	68	54	51	57
Nd	9.4	12.8	34.5	27	18.4	16.6	17.1	22.1	22.1	26.4	26.1	25.8	28.6	20.4	27.1	147	20.2	228	187	170	194
Eu	0.94	1.27	1.87	2.08	1.16	1.25	1.37	1.07	1.15	1.27	1.36	1.41	1.55	1.22	1.21	1.65	1.09	8.15	7.33	6.65	7.72
Sm	2.59	3.73	7.89	7.47	4.01	4.38	4.27	4.32	4.59	5.42	5.32	5.57	5.91	4.27	4.93	16.9	4.33	33.4	28.3	25	29.1
Gd	2.96	4.45	6.33	8.49	4	4.93	4.60	3.68	4.03	4.74	4.7	5.24	5.43	3.7	3.74	9.71	3.77	18.3	16.1	14.3	17.2
Tb	0.49	0.76	0.81	1.41	0.63	0.84	0.77	0.54	0.58	0.71	0.72	0.81	0.83	0.54	0.51	1.09	0.57	1.89	1.7	1.53	1.84
Dy	3.08	4.69	4.35	8.65	3.82	5.2	4.65	3.1	3.13	4.11	4.25	4.76	4.98	3.02	2.7	5.21	3.23	8.13	7.34	6.71	8.03
Ho	0.68	1.03	0.82	1.89	0.83	1.14	1.02	0.65	0.61	0.86	0.92	1.01	1.08	0.6	0.51	0.97	0.66	1.35	1.23	1.12	1.36
Er	1.94	2.87	2.11	5.29	2.35	3.25	2.87	1.8	1.58	2.4	2.58	2.8	3.04	1.56	1.33	2.45	1.78	3.25	2.94	2.69	3.25
Tm	0.3	0.43	0.33	0.8	0.37	0.5	0.44	0.28	0.23	0.37	0.4	0.43	0.48	0.23	0.19	0.36	0.27	0.46	0.41	0.37	0.45
Yb	1.98	2.8	2.32	5.28	2.56	3.28	2.9	1.94	1.49	2.44	2.71	2.86	3.21	1.43	1.25	2.25	1.78	2.94	2.54	2.44	2.92

(Continued)

Table 1. (Continued).

	Samanli				Iznik			Bigadic										Golcuk			
Sample	1wav	3wav	4wav	5wav	7wav	8wav	9wav	10wav	12wav	13wav	14wav	15wav	16wav	17wav	18wav	19wav	20wav	40wav	41wav	42wav	44wav
Tm	0.3	0.43	0.33	0.8	0.37	0.5	0.44	0.28	0.23	0.37	0.4	0.43	0.48	0.23	0.19	0.36	0.27	0.46	0.41	0.37	0.45
Yb	1.98	2.8	2.32	5.28	2.56	3.28	2.9	1.94	1.49	2.44	2.71	2.86	3.21	1.43	1.25	2.25	1.78	2.94	2.54	2.44	2.92
Lu	0.3	0.41	0.3	0.78	0.39	0.49	0.43	0.29	0.21	0.36	0.41	0.42	0.48	0.2	0.18	0.32	0.25	0.40	0.34	0.31	0.4
Hf	1.88	2.52	18.3	5.93	3.38	3.48	3.27	3.73	1.33	3.38	4.07	4.18	4.58	1.2	1.22	1.22	1.52	11.5	9.8	17.2	18.6
Ta	0.16	0.26	2.55	0.46	0.32	0.44	2.8	0.9	1.19	0.68	0.69	0.7	0.75	1.19	1.18	1.15	1.31	3.77	2.8	4.88	5.08
Pb	5.62	3.81	122	7.47	12.0	4.38	4.59	42.1	31.6	27.9	49	29.2	38.2	35.1	29.6	29.2	33.2	61	47.2	49.6	44.1
Th	1.41	1.61	64	3.62	5.25	3.09	2.89	17.9	14.1	13.7	12.9	11.1	13.1	13.1	17.2	81	15.1	104	59	74	69
U	0.5	0.41	21	1.13	1.34	0.51	0.73	6.05	2.6	3.42	3.53	2.99	3.37	3.58	4.36	4.61	4.41	21.3	13.1	11	5.43
$La/Sm_{(N)}$	1.72	1.35	2.43	1.47	3.91	1.95	2.08	4.27	3.76	3.75	3.7	3.33	3.79	3.81	4.94	11.4	3.56	6.36	5.6	6.76	6.08
Eu/Eu^*	1.03	0.95	0.81	0.8	0.89	0.82	0.94	0.82	0.82	0.76	0.83	0.79	0.83	0.94	0.86	0.39	0.82	1.01	1.05	1.08	1.05
Th/Yb	0.71	0.57	27.7	0.69	2.05	0.94	1	9.24	9.44	5.62	4.77	3.87	4.07	9.14	13.8	36	8.52	35.3	23.1	30.2	23.7
Ta/Yb	0.08	0.09	1.10	0.09	0.12	0.13	0.96	0.46	0.8	0.28	0.25	0.25	0.23	0.83	0.95	0.51	0.74	1.28	1.1	2	1.74
Ce/Pb	2.8	5.21	0.52	5.88	3.59	6.93	7.15	1.32	1.55	2.24	1.26	1.98	1.71	1.35	2.45	18	1.43	10.2	10.2	9.8	11.9

	Senir-kent	Afyon				Kirka	Seyitgazi		Simav				Kula						
Sample	39wav	33wav	35wav	37wav	45wav	46wav	47wav	48wav	21wav	22wav	23wav	24wav	26wav	27wav	28wav	29wav	30wav	31wav	32wav
SiO_2	45.7	61.5	60.5	60.4	59.7	77.2	51.2	51.3	58.4	57.8	59.8	60.3	47.8	47.8	47.5	48.4	49	46.9	48.5
Al_2O_3	14	16	14.4	14.5	16.5	12	15.6	16.5	16.6	15	16.6	17.2	17.8	18.7	18	18.5	18	17.4	16.9
Fe_2O_3	9.97	4.76	5.53	5.95	5.36	0.60	7.14	8.03	5.32	6.68	6.21	5.36	7.81	7.7	8.16	7.98	8.13	8.01	8.6
MnO	0.18	0.09	0.07	0.07	0.05	0.01	0.12	0.12	0.11	0.36	0.09	0.07	0.14	0.14	0.15	0.15	0.15	0.14	0.16
MgO	3.64	2.4	2.4	2.77	1.82	0.1	5.71	5.05	3.23	1.89	2.55	2.16	6.67	5.93	4.83	4.6	4.76	5.76	5.31
CaO	8.93	4.96	4.43	5.51	4.20	0.55	7.88	6.65	6.32	4.78	6.2	4.85	8.1	7.51	7.74	8.01	7.77	9.11	7.78
Na_2O	1.67	4	3.36	3.63	3.65	2.03	2.85	3.78	3.17	2.56	3.37	3.54	5.36	5.67	5.94	5.87	5.59	5.91	5.4
K_2O	7.85	3.90	5.68	4.53	4.48	4.78	3.85	3.35	2.55	5.59	2.26	4.25	3.44	3.74	3.25	1.79	3.7	2.1	3.19
TiO_2	1.62	0.59	0.73	0.82	0.89	0.04	1.4	1.25	0.74	1.01	0.62	0.71	1.83	1.73	1.85	1.85	1.85	1.99	1.92
P_2O_5	0.66	0.56	0.55	0.55	0.46	0.03	0.56	0.6	0.22	0.48	0.16	0.32	0.74	0.78	0.76	0.75	0.77	0.75	0.65
	5.6	0.8	0.9	1.1	1.90	2.5	2.8	2.50	2.2	3.90	2.1	1.2	0.2	0.2	1.7	2.1	0.1	2	0.4
Rb	546	115	173	156	141	356	114	83	124	189	67	138	79	74	90	23.1	85	38.7	73
Sr	1877	1343	1431	1883	1433	23.2	818	1266	629	1035	519	965	978	844	1002	809	885	835	923
Y	35	19.9	21.6	20.0	20.2	50	27.1	30.1	26.9	27.7	23.8	33	26.5	22.9	31.2	23.2	27.5	22.5	25.1
Zr	877	109	150	176	205	59	400	285	166	408	124	248	233	216	327	241	289	207	238
Nb	59	22.4	25	32.9	29.7	41.2	36.9	28.9	13.2	39.2	10.8	26.9	115	104	137	102	121	102	100

Ba	1537	1308	2780	2522	1793	26.1	533	1526	1354	1378	957	1305	943	864	916	1287	822	874	1112
La	30.6	63	59	77	74	12.1	28.4	84	37	74	31.7	77	48.9	45.3	54	43.9	49.6	46	54
Ce	62	123	108	137	138	17.7	59	164	71	147	61	142	86	81	101	81	92	84	99.2
Pr	7.5	13.8	12.2	14.9	15.5	3.48	7.01	18.6	7.9	16.5	6.89	15.5	9.51	8.81	11.2	8.99	10.2	9.33	10.9
Nd	33.8	49.7	43.9	52	54.1	14.3	29.1	68	28.8	59	25.5	54	34.8	31.7	41.2	32.9	37.5	33.7	39
Eu	1.86	1.95	2.09	2.35	2.1	0.17	1.37	3.03	1.38	2.35	1.21	2.15	2.2	1.9	2.5	2.01	2.26	2	2.21
Sm	7.75	8.2	8.02	8.73	8.81	4.92	5.75	11.8	5.84	10.4	5.17	9.43	6.83	6.01	8.05	6.38	7.26	6.50	7.31
Gd	6.18	5.47	5.81	5.84	5.84	5.36	4.72	8.32	5.07	7.47	4.52	7.24	6	5.24	6.95	5.43	6.26	5.53	6.07
Tb	0.8	0.67	0.75	0.72	0.72	1	0.63	1.04	0.75	0.93	0.67	0.96	0.87	0.75	1	0.78	0.9	0.78	0.86
Dy	4.32	3.39	3.81	3.60	3.61	6.28	3.57	5.25	4.3	4.66	3.92	5.24	4.8	4.1	5.49	4.26	4.9	4.22	4.65
Ho	0.82	0.64	0.71	0.66	0.67	1.33	0.71	1	0.9	0.87	0.83	1.05	0.94	0.81	1.09	0.85	0.97	0.83	0.91
Er	2.12	1.67	1.82	1.7	1.71	3.91	1.91	2.6	2.44	2.21	2.26	2.85	2.45	2.14	2.85	2.22	2.57	2.11	2.37
Tm	0.33	0.24	0.26	0.25	0.25	0.66	0.29	0.38	0.38	0.33	0.35	0.43	0.36	0.31	0.42	0.32	0.38	0.3	0.35
Yb	2.35	1.63	1.7	1.62	1.64	4.76	2.01	2.49	2.53	2.15	2.33	2.9	2.29	2.05	2.72	2.09	2.47	1.94	2.19
Lu	0.31	0.23	0.23	0.22	0.22	0.7	0.27	0.35	0.37	0.29	0.34	0.41	0.33	0.29	0.39	0.3	0.35	0.27	0.31
Hf	18.4	3.20	4.39	4.91	5.51	2.94	8.4	6.01	4.14	10.4	3.38	6.53	4.6	4.15	6.27	4.72	5.6	4.08	4.75
Ta	2.68	1.46	1.77	2.31	1.81	5.05	1.84	1.54	0.93	2.15	0.82	1.52	5.51	5.08	6.99	5.31	6.29	5.05	5.23
Pb	128	40.2	50	60	39.8	71	15.8	17.8	39.9	43.3	26	35.4	4.07	4.51	4.71	3.61	4.42	4.39	5.07
Th	7	31	40.9	57	35.5	41.9	16.4	21	19.6	40.1	14	30.7	7.97	7.67	9.45	7.29	8.77	7.43	8.04
U	22.9	10.3	11.8	16.9	11.2	15.8	4.4	4.68	5.5	10.3	3.5	8.86	2.21	2.16	2.68	1.9	2.46	1.96	2.26
$La/Sm_{(N)}$	2.49	4.81	4.60	5.52	5.29	1.54	3.11	4.46	3.99	4.46	3.86	5.14	4.5	4.75	4.24	4.33	4.3	4.45	4.62
Eu/Eu^*	0.82	0.89	0.93	1.01	0.9	0.1	0.8	0.93	0.77	0.81	0.76	0.8	1.05	1.04	1.02	1.04	1.02	1.02	1.02
Th/Yb	29.7	19.1	24	35.1	21.7	8.8	8.18	8.42	7.75	18.7	6.01	10.6	3.48	3.75	3.47	3.49	3.55	3.83	3.66
Ta/Yb	1.14	0.9	1.04	1.42	1.11	1.06	0.92	0.62	0.37	1	0.35	0.52	2.41	2.48	2.57	2.54	2.54	2.60	2.38
Ce/Pb	0.48	3.06	2.15	2.27	3.46	0.25	3.75	9.2	1.78	3.4	2.33	4.01	21.2	18	21.3	22.5	20.9	19.2	19.6

Note: Eu-anomaly (Eu/Eu^*) is defined as $Eu_{(N)}/\sqrt{Sm_{(N)} \times Gd_{(N)}}$ (Rollinson 1993). See Appendix 1 for details.

Table 2. Present-day Rb-Sr, Sm-Nd, U-Th-Pb isotope systematics of the studied Western Anatolian volcanic rocks.

Locality	Sample	Rb/Sr	$^{87}Sr/^{86}Sr(0)$	Sm/Nd	$^{143}Nd/^{144}Nd(0)$	$\varepsilon_{Nd(0)}$	U/Pb	Th/Pb	$^{206}Pb/^{204}Pb$	$^{207}Pb/^{204}Pb$	$^{208}Pb/^{204}Pb$
01-wav	Samanli-Dag	0.02	0.704367	0.275	0.512945	6.0	0.09	0.25	18.672	15.646	38.749
03-wav		0.02	0.704190	0.292	0.512883	4.8	0.11	0.42	18.685	15.632	38.738
04-wav		0.32	0.706223	0.229	0.512682	0.9	0.17	0.53	18.904	15.752	39.154
05-wav		0.02	0.704224	0.277	0.512968	6.4	0.15	0.48	18.718	15.646	38.763
07-wav	Iznik–Mudanya	0.05	0.705396	0.218	0.512814	3.4	0.11	0.44	18.635	15.594	38.610
08-wav		0.02	0.705380	0.264	0.512838	3.9	0.12	0.71	18.638	15.640	38.784
09-wav		0.03	0.704593	0.250	0.512766	2.5	0.16	0.63	18.709	15.632	38.753
10-wav	Bigadic-Sindigri	0.18	0.707327	0.195	0.512422	−4.2	0.14	0.42	18.896	15.702	39.032
12-wav		0.33	0.709055	0.208	0.512391	−4.8	0.08	0.45	18.879	15.742	39.185
13-wav		0.12	0.707403	0.205	0.512414	−4.4	0.12	0.49	18.709	15.684	39.009
14-wav		0.09	0.707676	0.204	0.512454	−3.6	0.07	0.26	18.776	15.755	39.295
15-wav		0.14	0.708077	0.216	0.512485	−3.0	0.10	0.38	18.798	15.753	39.201
16-wav		0.12	0.707431	0.206	0.512556	−1.6	0.09	0.34	18.803	15.746	39.194
17-wav		0.29	0.709077	0.210	0.512337	−5.9	0.10	0.37	18.919	15.785	39.322
18-wav		0.30	0.709221	0.182	0.512340	−5.8	0.15	0.58	18.939	15.783	39.296
19-wav		0.32	0.709096	0.115	0.512339	−5.8	0.16	2.78	18.842	15.688	39.008
20-wav		0.37	0.709216	0.214	0.512553	−1.7	0.13	0.46	18.826	15.666	38.938
40-wav	Golcuk–Isparta	0.01	0.703611	0.146	0.512726	1.7	0.35	1.69	19.014	15.764	39.292
41-wav		0.02	0.703527	0.151	0.512766	2.5	0.28	1.24	19.115	15.698	39.034
42-wav		0.01	0.703641	0.147	0.512736	1.9	0.22	1.49	18.768	15.735	39.179
44-wav		0.00	0.703645	0.150	0.512760	2.4	0.12	1.56	19.088	15.712	39.231
39-wav	Senirkent	0.29	0.706284	0.229	0.512697	1.2	0.18	0.54	18.907	15.759	39.147
33-wav	Afyon–Suhut	0.09	0.705644	0.165	0.512537	−2.0	0.26	0.77	19.002	15.771	39.234
35-wav		0.12	0.706385	0.183	0.512544	−1.8	0.23	0.81	18.903	15.763	39.145
37-wav		0.08	0.705219	0.168	0.512612	−0.5	0.28	0.94	18.924	15.650	38.863
45-wav		0.10	0.705832	0.163	0.512497	−2.8	0.28	0.89	18.969	15.762	39.211
46-wav	Kirka	15.32	0.707450(T) 0.720358(0)	0.345	0.512313	−6.3	0.22	0.59	19.070	15.855	39.630
47-wav	Seyitgazi	0.14	0.706446	0.198	0.512509	−2.5	0.28	1.04	19.014	15.683	39.080
48-wav		0.07	0.706151	0.174	0.512534	−2.0	0.26	1.18	19.101	15.741	39.298
21-wav	Simav–Usak	0.20	0.708469	0.203	0.512379	−5.1	0.14	0.49	19.014	15.764	39.292
22-wav		0.18	0.707162	0.176	0.512386	−4.9	0.24	0.93	19.115	15.698	39.034
23-wav		0.13	0.707470	0.202	0.512458	−3.5	0.13	0.54	18.768	15.735	39.179
24-wav		0.14	0.706584	0.176	0.512481	−3.1	0.25	0.87	19.088	15.712	39.231
26-wav	Kula	0.08	0.703150	0.196	0.512931	5.7	0.54	1.96	18.746	15.620	38.599
27-wav		0.09	0.703111	0.189	0.512943	5.9	0.48	1.70	18.719	15.594	38.496
28-wav		0.09	0.703217	0.195	0.512962	6.3	0.57	2.01	18.928	15.633	38.674
29-wav		0.03	0.703269	0.194	0.512950	6.1	0.53	2.02	18.904	15.595	38.606
30-wav		0.10	0.703148	0.194	0.512894	5.0	0.56	1.99	18.888	15.603	38.612
31-wav		0.05	0.703217	0.193	0.512946	6.0	0.45	1.69	18.850	15.633	38.733
32-wav		0.08	0.703301	0.187	0.512697	1.2	0.44	1.58	18.754	15.605	38.611

Note: For the Kirka sample 46-WAV, initial $^{87}Sr/^{86}Sr$ is also shown. See Appendix 1 for details.

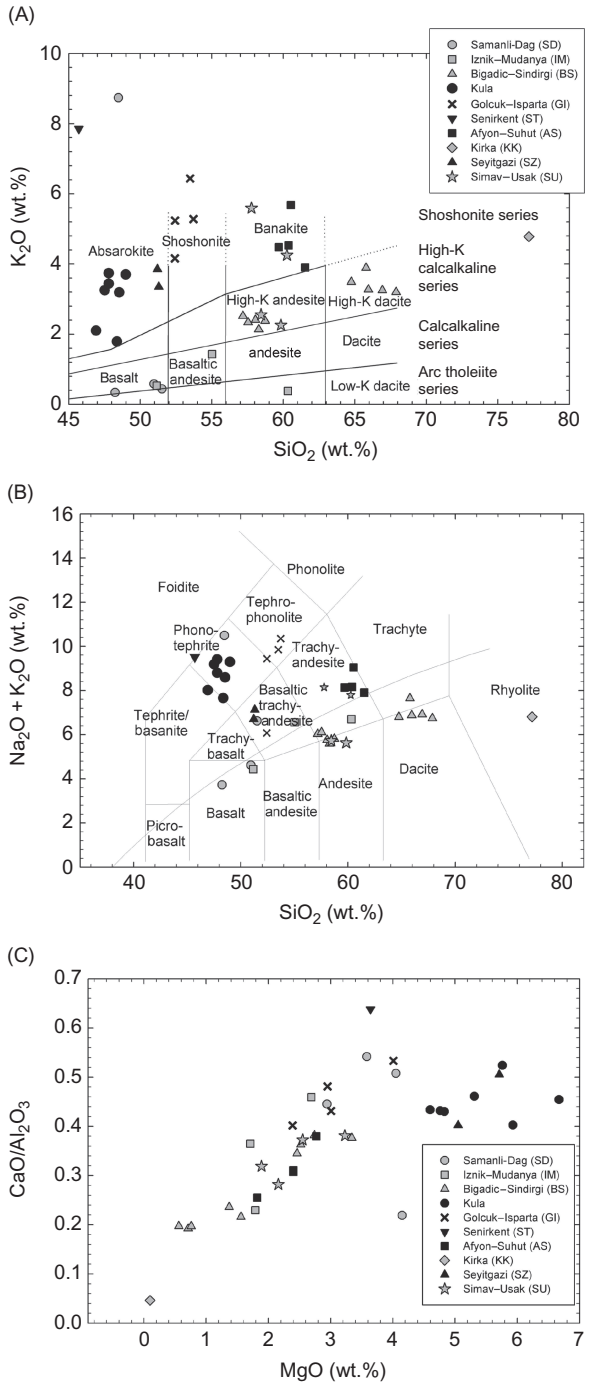

Figure 2. (A) Variation of K_2O versus SiO_2 (Peccerillo and Taylor 1976) and (B) total alkali silica diagram (Le Bas *et al*. 1991) showing the 10 different volcanic domains from Western Anatolia analysed in this study. Samanli-Dag, Iznik–Mudanya (north of the IAESZ), Bigadic–Sindirgi, and Kirka volcanics are dominantly calc-alkaline (grey) whereas the volcanics from the KAI trend including Golcuk–Isparta, Afyon–Suhut, Senirkent, as well as Seyitgazi and Kula are dominantly alkaline (black). Note the compositional bimodality in the Bigadic and Simav–Usak volcanics. (C) Plot of CaO/Al_2O_3 versus MgO (wt.%) showing an overall positive correlation suggesting the effect of clinopyroxene fractionation. Although the overall trends are not due to cogenetic fractional crystallization, the individual groups or lava suites may be affected by crystal fractionation.

with tuff, agglomerates, and lacustrine sedimentary rocks (Savascin and Oyman 1998). The Senirkent volcanic domain, with no available age data, is located within the apex of the IA, along the northeastern extension of the Burdur Fault Zone (Figure 1B). The Golcuk–Isparta volcanics occur farther south within the IA and range in age from 4.6 to 4.0 million years (Savascin and Oyman 1998). Kirka, Afyon–Suhut, and Golcuk–Isparta volcanics are hosted on the carbonates and rift assemblages of the Taurides whereas the Senirkent lavas occur within flysch deposits. These four volcanic domains occur along the N–S-oriented Kirka–Afyon–Isparta (KAI) structural trend within the Tauride block (Savascin and Oyman 1998). Except the solitary rhyolitic Kirka sample that represents one of the older volcanics in this region, the other KAI volcanics are mostly alkaline and belong to the shoshonitic series (Figure 2A and 2B). Senirkent shows the highest K_2O and lowest SiO_2 (Table 1). The Kirka Rhyolite shows low trace element concentrations and a prominent negative Eu-anomaly [$Eu/Eu^* = Eu_{(N)}/\sqrt{Sm_{(N)} \times Gd_{(N)}}$] (Rollinson 1993) (Table 1, Figure 3). The Afyon, Senirkent, and Isparta volcanics show uniform LREE-enriched patterns with prominent depletions of Nb and Ta with respect to the LILEs (Figure 3). The trace element concentrations of the Isparta volcanics (e.g. La$\sim$1000$\times$ chondrite) are higher than any other volcanics of this study; these volcanics are also compositionally different from the other volcanics along the KAI trend in having fractionated $La/Yb_{(\tilde{N})}$, high Ce/Pb (Figure 4), relatively depleted Nd–Sr isotopic composition as well as very low Rb/Sr (Figure 5), and the most radiogenic $^{206}Pb/^{204}Pb$ (Figure 6) compared with all the volcanics of this study.

Geochemically bimodal and akin to both the Afyon–Suhut and Bigadic–Sindirgi volcanics (e.g. Figures 2, 4B and 4D) are the calc-alkaline to shoshonitic Simav–Usak volcanics that are inferred to be of middle to upper Miocene age (Seyitoglu et al., 1997). These andesitic and trachyandesitic lavas are hosted within the Menderes metamorphic massif and show LREE enrichment and negative Nb–Ta anomalies (Figure 3). The Menderes metamorphic massif, thought to be an incipient core complex (Bozkurt and Park 1994), represents lower crustal units that were rapidly exhumed between 17 and 24 Ma (Okay and Satir 2002; Catlos and Cemen 2005). The Afyon volcanics show wide-ranging Ba/La, high Th/Yb, and arc-like Ce/Pb ratios (Figure 4) as well as relatively enriched Nd–Sr isotopes, high Rb/Sr (Figure 5), and radiogenic Pb isotopic (Figure 6) composition.

Also hosted within the Menderes massif are the young alkaline (phonotephrite) Kula volcanics, which are geochemically and isotopically distinct from the other volcanics of this study. They occur mainly as fissure eruptions at the intersection of the prominent grabens (Alici et al. 2002) and include the youngest mafic lavas in the region ($\sim$7.5–0.025 Ma). These volcanics show high MgO (4.6–6.67 wt.%) (Figure 2C), enrichments in LREE, LILE, as

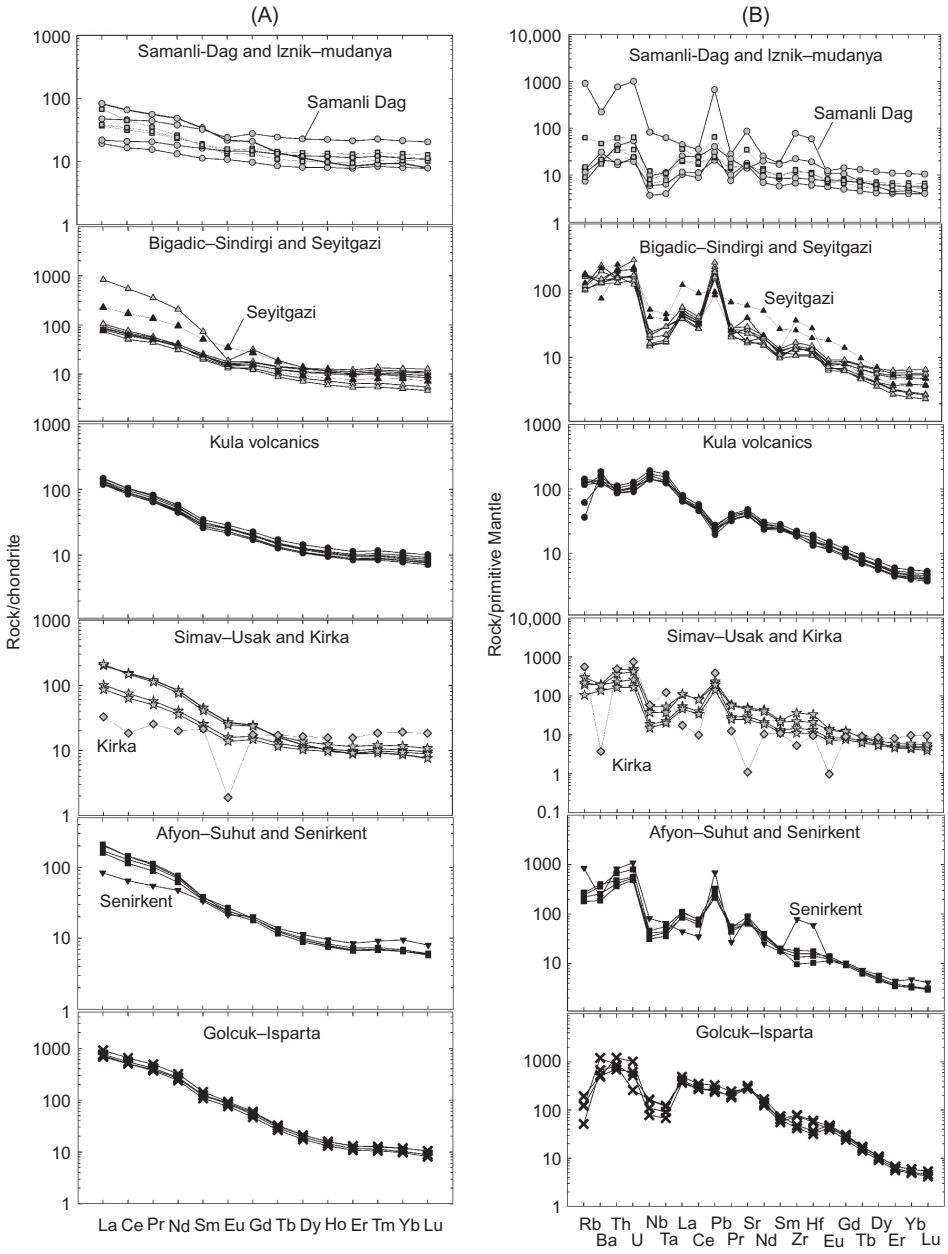

Figure 3. (A) Chondrite-normalized REE patterns and (B) primitive mantle-normalized 'spider' plots for all the volcanics of this study. All the volcanics show an overall LREE-enriched pattern. Note the prominent Nb and Ta depletions in most of the volcanics of this study indicative of their origin in a subduction zone environment. The Kula volcanics are compositionally different and show OIB-like trace element patterns. Symbols are the same as in Figure 2.

well as HFSE with no Nb–Ta anomaly and a negative Pb anomaly in primitive mantle-normalized trace element plots (Figure 3). Along with mantle-like high Ta/Yb and Ce/Pb (Hofmann et al. 1986) (Figure 4), Kula volcanics also show some of the most depleted Nd–Sr isotopic compositions ($\varepsilon_{Nd(0)}$ as high as +6.3), low but varying Rb/Sr (Figure 5), and the least radiogenic Pb isotopes among all the volcanics of this study (Figure 6).

4. Discussion of geochemical results: chemical geodynamics of Western Anatolia

In this section, we recapitulate and discuss the salient aspects of the petrogenesis of the lavas that can be inferred from the geochemical data as presented above. These inferences are then utilized in reconstructing the geodynamic evolution of Western Anatolia. As mentioned already, Cenozoic volcanism in Western Anatolia has evolved

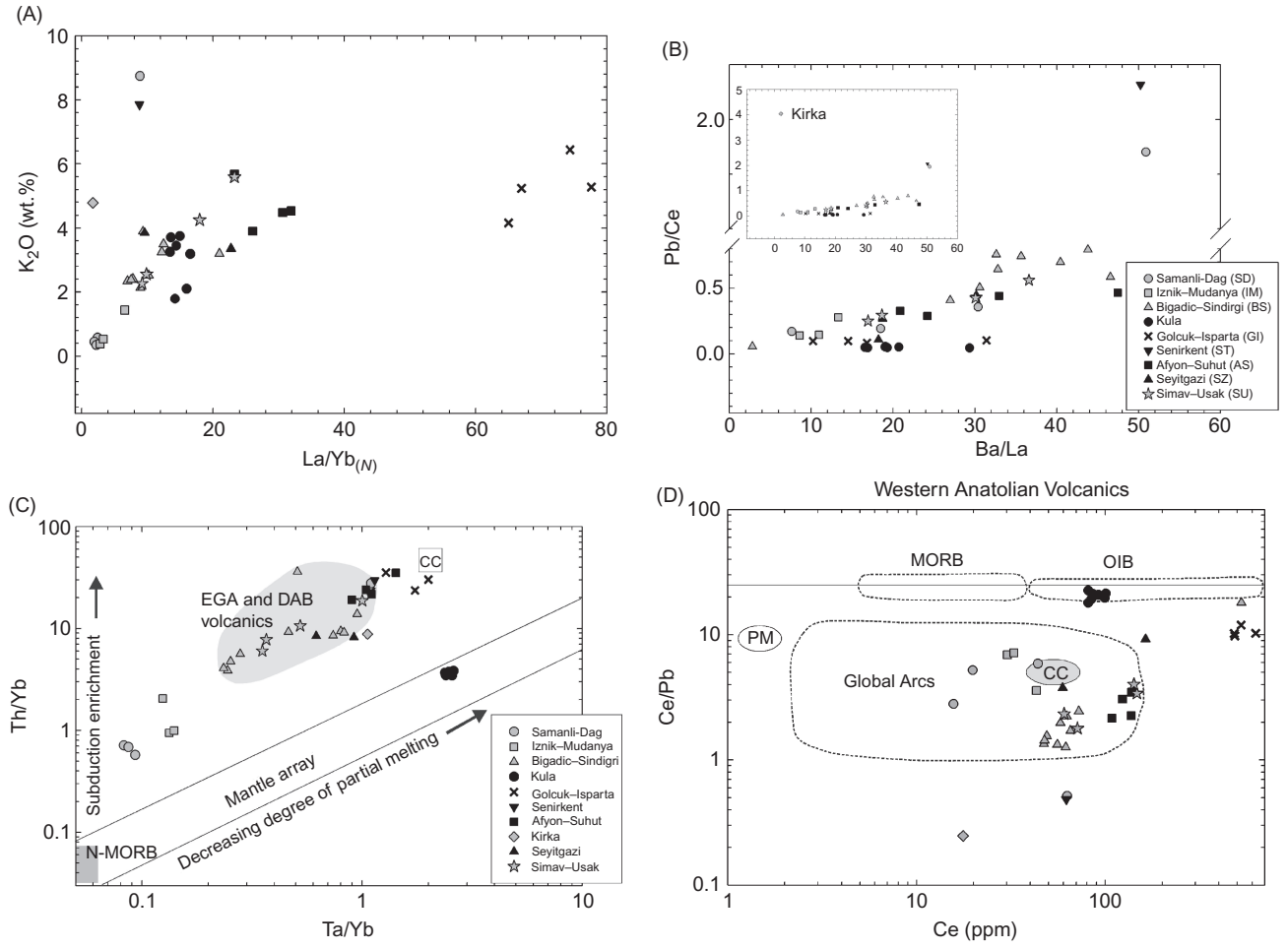

Figure 4. (A) K_2O (wt.%) increases with chondrite-normalized La/Yb, a proxy for the degree of partial melting, suggesting that high K_2O (wt.%) observed in some volcanics of this study is a result of low-degree partial melting. (B) A positive correlation between Pb/Ce and Ba/La for most of the above volcanics also suggests fluid infiltration, where Pb and Ba are both fluid-mobile elements. The Kula and Golcuk volcanics fall off this trend. (C) Variation of Th/Yb versus Ta/Yb for the Western Anatolian volcanics. Also shown are the domains of N-MORB, the mantle array, and the average continental crust (CC). The Kula volcanics plot on the mantle array whereas the Samanli and Iznik volcanics (north of IAESZ) plot slightly above this array but with low Ta/Yb. All other volcanics show much higher Th/Yb as well as Ta/Yb indicating enrichment by subduction fluids (high Th/Yb) and the lithospheric mantle (high Ta/Yb) (Pearce 1983) and also overlap with the EGA and DAB volcanics (Aldanmaz et al. 2000) of northwest Anatolia, which are also believed to have formed in an arc setting. (D) A plot of Ce/Pb versus Ce concentration (ppm) showing the domains of MORBs, OIBs, primitive mantle (PM), continental crust (CC), and global arcs (Hofmann *et al*. 1986; Miller *et al*. 1994). Ce/Pb of the Kula volcanics (open symbols) overlaps with the composition of oceanic basalts whereas Ce/Pb of the SD-IM-BS volcanics (grey) to the north of the IAESZ as well as the Isparta region volcanics (dark) broadly overlaps with the composition of global arcs.

from calc-alkaline and acidic to dominantly mafic, alkaline compositions (Yilmaz 1989; Savascin 1990; Yilmaz 1990; Seyitoglu et al. 1997; Yilmaz et al. 2001; Akay and Erdogan 2004; Altunkaynak and Genc 2008). This bimodal composition is also observed in volcanics within single basins, for example the Selendi Basin (Figure 1B) (Ersoy and Helvaci 2007; Ersoy et al. 2008). The initial calc-alkaline volcanism in Western Anatolia was not related to any active subduction occurring at that time, although the influence of older subduction systems in modifying the magma source composition cannot be ruled out. Among the 10 different volcanic domains described in this study, all volcanics other than Kula share certain geochemical signatures mostly indicating the influence of subduction zone fluids. These calc-alkaline and alkaline volcanics show an overall positive correlation between CaO/Al_2O_3 and MgO (Figure 2C), suggesting clinopyroxene fractionation during the genesis of these lavas. In addition, these volcanics show LREE enrichment, negative Nb–Ta anomalies (Figure 3), and a positive correlation between Pb/Ce and Ba/La, Th/Yb and Ta/Yb, as well as K_2O and $La/Yb_{(N)}$ (Figure 4). Also notable is the overall positive correlation between present-day $^{87}Sr/^{86}Sr$ and Rb/Sr ratios (Figure 5B). The compositions of some of

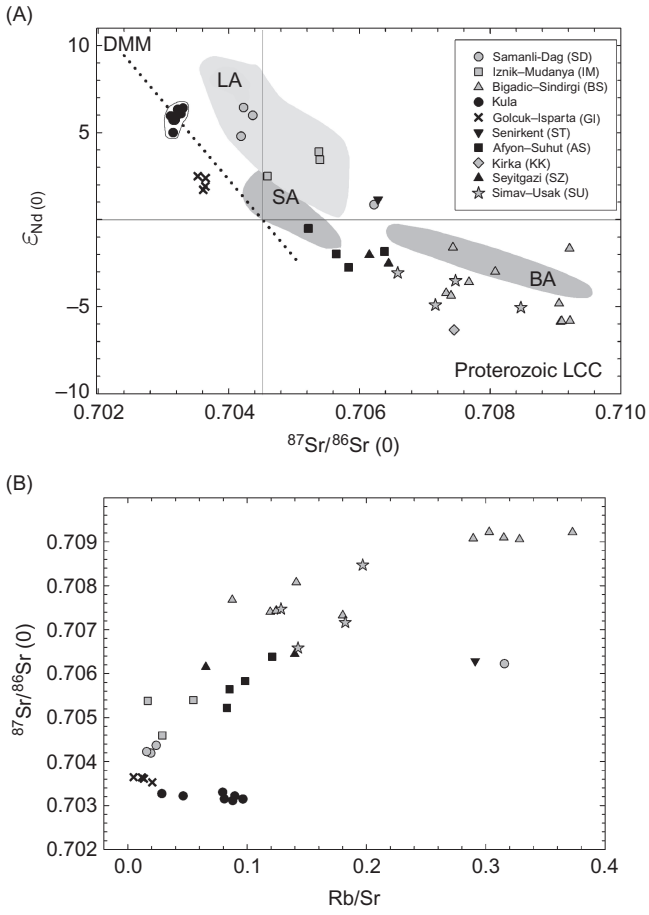

Figure 5. (A) Present-day Nd–Sr isotopic composition of the Western Anatolian volcanics. Also shown for comparison are the domains of the depleted MORB mantle (DMM), Proterozoic lower continental crustal rocks (LCC), and arc volcanics from the Lesser Antilles (LA) (http://georoc.mpch-mainz.gwdg.de/; Hawkesworth *et al*. 1979a, 1979b; Hawkesworth and Powell 1980), Sunda arc (SA) and the Banda arc (BA) (http://georoc.mpch-mainz.gwdg.de/; Whitford *et al*. 1981). The single Kirka sample has unusually high Rb/Sr values and hence its initial Sr isotopic composition at 21 Ma (Savascin 1990) is plotted (see text for details). (B) The Western Anatolian volcanics of this study show a rough positive correlation between present-day Sr isotopic composition and Rb/Sr ratio. Kirka has the highest Rb/Sr ratio and plots outside the shown range. The Samanli and Iznik volcanics from north of the IAESZ, the Golcuk volcanics, and the Kula volcanics show the least Rb/Sr.

these volcanics are representative of interactions of the upwelling magma with different basement rocks.

4.1. Samanli-Dag and Iznik–Mudanya volcanics (north of the IAESZ)

Geochemical and isotopic data on the Samanli and Iznik volcanics, located to the north of the IAESZ (Figure 1B), are sparse and this study attempts to improve our understanding of these important rocks with the help of geochemical characteristics in the context of the geodynamic evolution of Western Anatolia. There are no age

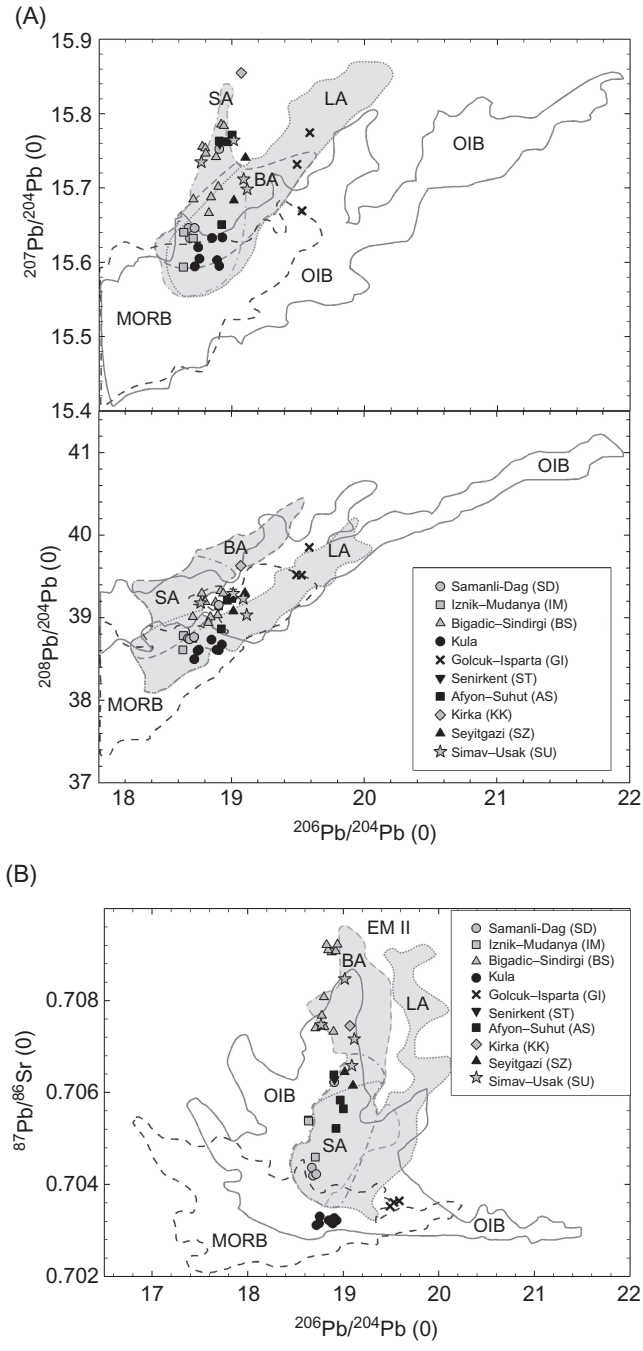

Figure 6. (A) Present-day Pb isotopic composition of the volcanics of this study. Also shown are the domains of MORBs, OIBs, as well as volcanics from the Banda arc, Sunda arc, and Lesser Antilles (http://georoc.mpch-mainz.gwdg.de/). Most of the volcanics overlap with the compositions of the arc-derived magmas mentioned above. Kula volcanics and the Samanli and Iznik volcanics (north of IAESZ) show the least radiogenic values and overlap with the composition of oceanic basalts. The high $^{207}Pb/^{204}Pb$ at low $^{206}Pb/^{204}Pb$ in the Bigadic lavas and the Isparta region volcanics suggests the involvement of old continental crustal material. (B) Present-day Sr–Pb isotope correlation diagram. The Kula, Samanli and Iznik, and Golcuk volcanics show the least radiogenic compositions and overlap with the compositions of oceanic basalts. Other volcanics of this study overlap with the compositions of Banda arc lavas (http://georoc.mpch-mainz.gwdg.de/).

estimates for these volcanics but their eruption age could be as old as the Oligo-Miocene based on their location north of the IAESZ and composition as described below.

The Samanli and Iznik volcanics are calc-alkaline with relatively low K_2O, ranging from basalts and basaltic andesites to basaltic trachyandesites, andesites, and dacites (Figure 2A and 2B) and are located on basement rocks comprising the Sakarya Continent and Karakaya Complex. In chondrite-normalized REE (rare earth element) plots (Figure 3A), the Samanli volcanics show the least fractionated LREE. A couple of Samanli samples show relatively flat REE patterns. Iznik volcanics also show uniform LREE enrichment. Most of the Samanli and Iznik volcanics show small negative Eu-anomalies (Table 1) (Rollinson 1993) indicating plagioclase fractionation in the magma chamber.

The Samanli and Iznik volcanics show prominent Nb–Ta depletions in primitive mantle-normalized trace element plots (Figure 3B) characteristic of arc-derived magmas formed by mantle-wedge melting (Tatsumi and Eggins 1995). Nb–Ta depletions are also observed in continental crustal rocks but other geochemical and isotopic signatures can clearly distinguish between arc magmas and continental crustal rocks. The Samanli and Iznik volcanics together show relatively low but wide-ranging Ba/La ratios (Figure 4B), characteristic of fluid influence in a subduction zone environment that is also attested by their Ce/Pb ratio (Figure 4D) that broadly overlaps with the compositions of global arcs (Miller et al. 1994). Both Ba and Pb are fluid-mobile elements and a positive correlation between Pb/Ce and Ba/La (Figure 4B) suggests the strong influence of fluids in the genesis of the Samanli and Iznik volcanics, similar to those observed in a subduction zone setting. Similar arc-like geochemical signatures have also been reported from other calk-alkaline volcanics in Northern Anatolia (Peccerillo and Taylor 1976).

The covariation of K_2O in each volcanic suite with $La/Yb_{(N)}$ values (Figure 4A) may be due to different degrees of partial melting; for example, lower degrees of partial melting are equated with higher K_2O contents and $La/Yb_{(N)}$ values. The Samanli and Iznik volcanics plot above the mantle array in a plot of Th/Yb versus Ta/Yb (Pearce 1983) (Figure 4C) indicating subduction enrichment, but their relatively low Ta/Yb rules out their derivation from a subduction-metasomatized lithospheric mantle (Pearce 1983).

Compared with other Miocene post-collisional volcanics of Western Anatolia, which show subduction enrichment only in their trace element concentration patterns, the Samanli and Iznik volcanics are unique in their relatively depleted Nd–Sr isotopic compositions with $\varepsilon_{Nd(0)}$ as high as +6.4 (5-WAV) and low Rb/Sr (Figure 5) as well as their unradiogenic Pb isotopic compositions (Figure 6) that overlap with those of MORBs and OIBs as well as arc lavas from Sunda, Banda, and the Lesser Antilles (Figures 5 and 6). This observation suggests the role of a depleted arc mantle in the generation of these lavas as these samples plot to the right of the Nd–Sr mantle array (Figure. 5A). This suggestion is also supported by the Pb isotopic ratios of these two groups as shown in Figure 6. The above-mentioned radiogenic Nd isotopic compositions also indicate minimal continental crustal contamination in these volcanics. In this context, it is interesting to mention the 12–6 million-year-old alkaline volcanics from the Thrace Basin, farther east, which also show very radiogenic Nd ($\varepsilon_{Nd(0)}$ as high as +6.3) but OIB-like trace element concentration patterns (Aldanmaz et al. 2006). Pb isotopic composition of Samanli and Iznik volcanics overlaps with the composition of MORBs and volcanics from the active Banda, Sunda, and Lesser Antilles arcs (http://georoc.mpch-mainz.gwdg.de/) (Figure 6A), which are generally believed to be derived by mantle-wedge melting. In a Sr–Pb isotope correlation diagram (Figure 6B), the Samanli and Iznik volcanics plot close to the composition of MORBs, representative of the depleted mantle.

Our geochemical data are consistent with a model involving partial melting of a metasomatized mantle-wedge that formed during subduction of the Neotethyan oceanic crust (Figure 7). This melting was followed by subsequent assimilation of variable amounts of basement rocks (although minimal), which is are consistent with the geochemical and isotopic signatures of the Samanli and Iznik volcanics as discussed above. Radiogenic Nd isotopes, in particular, indicate widespread occurrence of upwelling asthenosphere beneath this region and are consistent with similar observations in the Thrace Basin located farther east (Aldanmaz et al. 2006).

Any model attempting to explain the volcanism to the north of the IAESZ in Western Anatolia should take into account that volcanism in this region took place in a collisional setting after the cessation of the Late Cretaceous–middle Eocene northerly dipping subduction of the Neotethyan plate beneath the Sakarya Continent along the IAESZ (Okay et al. 1998; Aldanmaz et al. 2000). We suggest that the partial melting of the metasomatized Neotethyan mantle-wedge, long after active subduction, was facilitated by heat derived from asthenospheric upwelling, possibly resulting from delamination of the subducted Neotethyan slab allowing asthenospheric upwelling (Figure 7). Slab delamination has been invoked to explain the origin of I-type granitoids in northwestern Anatolia (Koprubasi and Aldanmaz 2004) as well as the central Aegean adakites (Pe-Piper and Piper 2001). Our Pb isotopic data are also compatible with the above model. It is interesting to note that previous studies on isolated calc-alkaline volcanics in Western Anatolia have also hinted for a subduction component in the source region of these volcanic rocks (Gulec 1991; Aldanmaz et al. 2000). However, our isotopic data strongly demonstrate the involvement of a depleted asthenospheric component in the genesis of these volcanics that has been modified by subduction

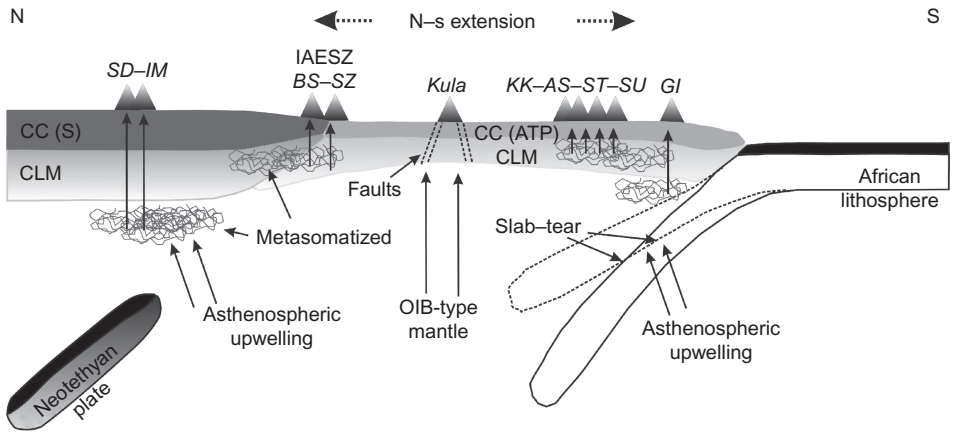

Figure 7. A schematic representation of the proposed petrogenetic models for the volcanics of this study including Samanli (SD) and Iznik (IM) located to the north of the IAESZ (see Figure 1B), the Bigadic (BS) and Seyitgazi (SZ) hosted within the suture zone, Kirka (KK), Afyon (AS), Senirkent (ST), Golcuk (GI), and Kula. Also shown are the Sakarya (S) and Anatolide–Tauride platform (ATP) continental crust (CC) and lithospheric mantle (CLM). See text for details.

zone metasomatism. It must be noted that the most convincing arc-like signatures observed in these rocks are the negative Nb–Ta anomalies and the Ce/Pb ratios. Th/Yb and Ba/La ratios in these volcanics are relatively low but consistent with arc-derived magmas. We suggest that the arc-component in these volcanics is relatively minor and most likely there is an arc contaminant in an asthenospheric source for these volcanics.

4.2. Bigadic–Sindirgi volcanics

The 23–15 million-year-old Bigadic–Sindirgi volcanics (Erkul et al. 2005) are hosted within the IAESZ and constitute an eastward extension of the calc-alkaline rocks in the Biga Peninsula (Aldanmaz et al. 2000; Altunkaynak and Genc 2008). These high-K calc-alkaline rocks show a compositional bimodality in major element (Figure 2), Nd–Sr–Pb isotopic compositions, and Rb/Sr ratios (Figures 5 and 6), possibly reflecting the nature of the basement assimilant, which are either ophiolites or carbonates within the suture zone. The above-mentioned compositional bimodality is not observed in the normalized trace element concentration patterns in Figure 3. One Bigadic sample (19-WAV) showing highly fractionated LREE and anomalously high La concentration (∼800× chondrite) occurs as a dike.

The Bigadic volcanics show overall uniform trace element concentration patterns with LREE enrichment and prominent negative Nb–Ta anomaly (Figure 3B) characteristic of arc-derived magmas formed by mantle-wedge melting (Tatsumi and Eggins 1995). Together with arc-like Ce/Pb ratios (Miller et al. 1994) (Figure 4D), these volcanics show a positive correlation between Pb/Ce and Ba/La (Figure 4B), where both Ba and Pb are fluid-mobile elements, indicating influence of subduction zone fluids in their genesis. The Bigadic volcanics plot above the mantle array in a plot of Th/Yb versus Ta/Yb (Figure 4C) indicating subduction enrichment and overlap with the compositions of the Ezine–Gulpinar–Ayvacik (EGA) and Dikili–Ayvalik–Bergama (DAB) volcanics located farther west, which are believed to have formed in an arc setting (Aldanmaz et al. 2000). Their high Ta/Yb suggests contribution from a lithospheric mantle source (Pearce 1983).

The Bigadic volcanics show unradiogenic Nd ($\varepsilon_{Nd(0)}$ values, as low as −6.3) and radiogenic Sr as well as high Rb/Sr (Figure 5), suggesting possible assimilation of the upper continental crustal rocks. Sr isotopes in these rocks are clearly more radiogenic than other volcanics of this study with similar Nd isotopic compositions (Figure 5) and they overlap with the compositions of other arc-derived magma (e.g. Banda arc) where similar radiogenic Sr is generally explained by the involvement of seawater-altered subducted oceanic crust (Hawkesworth 1979; Hawkesworth et al. 1979a, 1979b; Hawkesworth and Powell 1980; Whitford et al. 1981). Incorporation of subducted sediments can also result in the observed shift towards radiogenic Sr isotopic composition (DePaolo 1988) and is consistent with the high Th/La in these volcanics (0.26–0.62), which is considered to be a proxy of subducted sediments (Plank 2005). However, extensive sediment incorporation would also lower the Nd isotopic ratio, which is not observed in the Bigadic rocks.

Most of the Bigadic volcanics show high $^{207}Pb/^{204}Pb$ at low $^{206}Pb/^{204}Pb$ (Figure 6A), suggesting the involvement of old continental crustal material. Similar vertical trends are also observed in other arc-derived lavas from the Sunda arc. Bigadic volcanics also show overall high $^{208}Pb/^{204}Pb$ and overlap with the compositions of Banda

and Sunda arc lavas. In a Sr–Pb isotope correlation diagram (Figure 6B), these volcanics show radiogenic Sr and relatively constant Pb isotopes, suggesting contribution from an EM II-type mantle source.

4.3. Seyitgazi volcanics

The 6–11 million-year-old Seyitgazi volcanics located farther east of Bigadic–Sindirgi are also hosted within the IAESZ ophiolites. However, in contrast to the subalkaline composition of the Bigadic volcanics, the Seyitgazi rocks can be classified as absarokite (Figure 2A) and trachyandesites (Figure 2B), being enriched in the alkalism, and show relatively lower SiO_2 and higher MgO (Figure 2). They show LREE enrichment and Nb–Ta depletions (Figure 3) similar to arc volcanics derived from mantle-wedge melting. Compared with Bigadic–Sindirgi, the Seyitgazi volcanics show considerably lower Ba/La (Figure 4B) and Rb/Sr (Figure 5B) but show similarly high Th/Yb and Ta/Yb (Figure 4C), suggesting subduction enrichment, and overlap with the composition of the EGA and DAB volcanics, also formed in an arc setting (Aldanmaz et al. 2000) (Figure 4C). The Seyitgazi volcanics show Ce/Pb broadly similar to global arcs (Figure 4D), radiogenic $^{206}Pb/^{204}Pb$ (Figure 6), and enriched Nd–Sr isotopic composition (Figure 5A), although not as enriched as the Bigadic lavas. The isotopic composition of the Seyitgazi volcanics also broadly overlaps with arc lavas from Sunda, Banda, and the Lesser Antilles (Figures 5 and 6).

Overall, the geochemical and isotopic compositions of the Seyitgazi volcanics show a clear imprint of subduction zone fluids, although the enriched Nd–Sr and radiogenic Pb isotopic compositions as well as high Ta/Yb suggest involvement of the lithospheric mantle. Given that the time of eruption of these volcanics was long after any active subduction in this region, we suggest that these volcanics were derived from a subduction-modified lithospheric mantle during extensional tectonics (Figure 7).

4.4. Kirka, Afyon–Suhut, Golcuk–Isparta, and Senirkent volcanics

Kirka (21–17 Ma), Afyon–Suhut (14–8 Ma), Golcuk–Isparta (4.6–4.0 Ma), and Senirkent lavas (age not known) are hosted within the Tauride platform and occur along the N–S-oriented KAI structural trend (Savascin and Oyman 1998). Other than the solitary rhyolitic Kirka sample, these volcanics are mostly alkaline and belong to the shoshonitic series (Figure 2A and 2B). Senirkent shows the highest K_2O and lowest SiO_2, whereas the Golcuk and Afyon rocks show equally high Na_2O and K_2O (Table 1). The Kirka Rhyolite shows low trace element concentrations and a prominent negative Eu-anomaly (Figure 3A, Table 1), indicating plagioclase fractionation. The Afyon, Senirkent, and Golcuk volcanics show uniform LREE-enriched patterns and, as also observed in Kirka, prominent Nb–Ta depletions (Figure 3), indicating influence of subduction zone fluids. Subduction enrichment is also indicated by their high Th/Yb, whereas high Ta/Yb (Figure 4C) suggests contribution from the lithospheric mantle (Pearce 1983). Ce/Pb for the Afyon volcanics along the KAI trend overlaps with global arcs (Miller et al. 1994) (Figure 4D). However, the Golcuk volcanics, with arc-like Ce/Pb values, have much higher Ce contents because of their extreme LREE enrichment due to low-degree partial melting, consistent with their high $La/Yb_{(N)}$ (Figure. 4A). Low Ce/Pb in Kirka and Senirkent are possibly due to higher degree of continental crustal assimilation, as suggested by their non-radiogenic Nd isotopic signatures (Figure 5A).

Within some of these volcanic domains, variation in K_2O is correlated with the degree of partial melting. Samples with higher $La/Yb_{(N)}$, interpreted to indicate lower degrees of partial melting, show higher K_2O (Figure 4A). This trend is particularly observed in the Afyon and Golcuk volcanics. The Golcuk–Isparta volcanics compositionally stand out from the other volcanics along the KAI trend in having much higher trace element concentrations and $La/Yb_{(N)}$ (highest among all the volcanics of this study), higher Ce/Pb, relatively depleted Nd–Sr isotopic composition, very low Rb/Sr, and most radiogenic $^{206}Pb/^{204}Pb$ among all the volcanics of this study.

The relatively radiogenic Nd isotopic compositions ($\varepsilon_{Nd(0)} = +1.7$ to $+2.5$) of the Golcuk rocks (Figure 5A) are similar to those observed in typical arc lavas (Salters and Hart 1991) formed by melting of the mantle-wedge. In contrast, the Nd isotopic compositions of Kirka, and Afyon and Senirkent, also occurring along the KAI trend, are relatively enriched (Figure 5A) and can be interpreted by varying degrees of assimilation of the local basement rocks, which are carbonates and rift assemblages of the Taurides. The Senirkent volcanics show unusually radiogenic Sr isotopes compared with other volcanics with similar Nd isotopic compositions.

Most of these volcanics along the KAI trend show vertical enrichment trends in the Pb isotope plots (Figure 6) with high $^{207}Pb/^{204}Pb$, higher than those observed in MORB. The radiogenic $^{207}Pb/^{204}Pb$ suggests involvement of ancient continental crust in the genesis of these lavas. This ancient component could have been derived from assimilation of basement rocks. It is noteworthy that the Pb isotopic compositions of most of these volcanics overlap with Sunda and Banda arc volcanics (http://georoc.mpch-mainz.gwdg.de/). In the Sr–Pb isotopic space (Figure 6B), the contribution of an EM II-type mantle source is evident for the genesis of the KAI volcanics. Alternatively, this could also reflect assimilation of basement rocks. The overall vertical trend with wide-ranging Sr isotopes and less variation in Pb isotopes mimics the trend observed in

the Sunda and Banda arcs. The Golcuk volcanics show the most radiogenic $^{206}Pb/^{204}Pb$ (Figure 6A) among all the volcanics of this study indicating their derivation from a unique source that is different from those of the other volcanics from the KAI trend. In a Sr–Pb isotope correlation diagram (Figure 6B), the Golcuk volcanics overlap with the compositions of ocean island basalts.

Overall, the geochemical and isotopic compositions of the Kirka, Afyon, and Senirkent volcanics show clear imprint of subduction zone fluids although the enriched Nd–Sr and radiogenic Pb isotopic compositions as well as high Ta/Yb suggest involvement of the lithospheric mantle. Given that the time of eruption of these volcanics was long after any active subduction in this region, we argue that these volcanics were derived from a subduction-modified lithospheric mantle during extensional tectonics (Figure 7). The Golcuk volcanics, with relatively depleted Nd–Sr isotopes and characteristically different $^{206}Pb/^{204}Pb$ isotopic compositions similar to oceanic basalts, suggest contribution from a subduction-modified depleted mantle, possibly by low-degree decompressional melting of the asthenosphere during regional extension followed by subsequent assimilation of basement rocks. Alternatively, these volcanics could also be derived by low-degree melting of the lithospheric mantle metasomatized by subduction fluids and asthenospheric melts.

The involvement of an asthenospheric source in the genesis of the Golcuk lavas is also supported by our knowledge of the regional tectonic features in the Isparta region. The most important structural feature of the Isparta region is a major re-entrant known as the IA (Figure 1), which is formed by NE- and NW-trending oblique faults (Taylor and Nesbitt 1998). Seismic data indicate a neotectonic extensional regime in the outer edge of the IA (Kocyigit and Ozacar 2003). The N–S-oriented KAI trend (Figure 1B) is thought to represent a fault-controlled margin between Western Anatolia, which has a 30 mm/year southwesterly motion, and Central Anatolia, which moves in a westerly direction at 15 mm/year (Savascin and Oyman 1998; Taylor and Nesbitt 1998). This structural trend, although lacking any motion (Dilek and Moores 1990), is considered to be a regional discontinuity or transform fault between the Hellenic and Cyprean arcs. The NE-trending Burdur Fault and the roughly N–S-trending Akseher–Simav Fault (Figure 1B) are the continental extensions of the Hellenic and Cyprean arcs, respectively (Savascin and Oyman 1998). The Hellenic arc and the Pliny–Strabo Trench mark the boundary between the African and Eurasian plates in the west, whereas the Cyprus arc and other diffuse fault systems mark the boundary in the east (Taymaz et al. 1991; Doglioni et al. 2002; Tokcaer et al. 2005) (Figure 1A). The two arcs are perpendicular to the relative motion of Africa relative to Eurasia (Taylor and Nesbitt 1998).

Very low Pn velocities (<7.8 km/s) have been recorded beneath the IA and interpreted due to the absence of a lithospheric mantle lid beneath this region (McKenzie 1978). The occurrence of a low velocity zone in this region is also supported by magnetotelluric studies (Yagmurlu et al. 1997), which indicate high lower crustal conductivity along the Burdur Fault Zone, suggesting asthenospheric upwelling. In contrast, crustal conductance decreases drastically farther southeast in the IA indicating that the crust is relatively stable (Yagmurlu et al. 1997). The Hellenic arc is widely believed to be retreating due to the subduction rollback of the African plate whereas the Cyprean arc is relatively stationary (Barka et al. 1997) and the subduction angle beneath this arc is relatively shallow (Al-Lazki et al. 2004). Seismic tomography suggests that there is a tear between these two plate segments (Dilek and Moores 1990; Gurer et al. 2004). The KAI structural trend (Savascin and Oyman 1998) is possibly a manifestation of this tear in the subducting African lithosphere and may explain the mechanism for asthenospheric upwelling in this region. A similar slab-tear scenario has also been suggested for the genesis of lamproites in the Isparta region (Çoban and Flower 2007).

Based on our geochemical and isotopic data presented and discussed in this study, and taking into account the geophysical evidence summarized above, we propose a chemical geodynamic model in which the alkaline volcanics along the KAI structural trend in the Isparta region were influenced by subduction of the African lithosphere beneath the Anatolian Plate. Subduction-related metasomatism modified the source regions of the Kirka, Afyon, Senirkent, and Golcuk volcanics. Differences in subducting plate velocities along the Hellenic and Cyprean trenches resulted in a tear in the subducting African lithosphere. This slab window allowed asthenospheric upwelling that provided an additional heat source for melting of the mantle-wedge that formed the Golcuk volcanics (Figure 7).

4.5. Simav–Usak volcanics

Four Simav–Usak rock samples analysed in this study show bimodal geochemical compositions. Although two of these samples are calc-alkaline and akin to the Bigadic–Sindirgi lavas, the other two samples are alkaline and similar to the Afyon–Suhut volcanics. Even in other major elements, as well as trace element and isotopic compositions, the bimodality of the Simav–Usak lavas is clearly observed. Overall, the LREE-enriched Simav–Usak volcanics show arc-like geochemical characteristics including negative Nb–Ta anomalies (Figure 3B), positively correlated Pb/Ce and Ba/La, and high Th/Yb and Ce/Pb, similar to global arcs (Miller et al. 1994) (Figure 4).

These volcanics show enriched Nd–Sr isotopic compositions, high Rb/Sr like the Bigadic volcanics (Figure 5), and radiogenic Pb isotopic (Figure 6) compositions, which overlap with the compositions observed in the Sunda arc lavas. Overall, the geochemical and isotopic compositions

of the Simav–Usak volcanics show clear imprint of subduction zone fluids although the enriched Nd–Sr and radiogenic Pb isotopic compositions (Figures 5 and 6) as well as high Ta/Yb (Figure 4C) suggest derivation from a lithospheric mantle. As mentioned earlier, the Simav–Usak volcanics erupted long after any active subduction in this region. Hence, we argue that these volcanics were derived from a subduction fluid-metasomatized lithospheric mantle during later extensional tectonics (Figure 7). High $^{207}Pb/^{204}Pb$ indicates contribution from an old continental crustal component that is possibly the basement Menderes massif.

4.6. Kula volcanics

Among all the volcanics of this study, the Kula volcanics, which are the youngest rocks of this study, are compositionally unique and are located at the intersection of prominent grabens formed due to post-collisional extension (Figure 1B) (Alici et al. 2002). These alkalic (both high Na and K) and silica-undersaturated volcanics (Figure 2A) also show high CaO and MgO (Table 1) at lower SiO_2 and are hosted within the Menderes metamorphic massif.

Trace element concentration patterns of the Kula volcanics (Figure 3) are, in general, similar to ocean island basalts (Sun and McDonough 1989). Lack of any Nb–Ta anomaly (Figure 3B) and OIB-like Ce/Pb (Figure 4D) (Hofmann et al. 1986) suggests lack of continental crustal and fluid-enriched mantle-wedge components in these lavas, which is consistent with earlier studies of Kula volcanics (Seyitoglu et al. 1997). Similar trace element signatures have been reported for potassic lavas from the Denizli region (Yılmaz, 2010). In a plot of Th/Yb versus Ta/Yb (Figure 4C), these volcanics lie on the mantle array and do not show any subduction-related enrichments or contribution from the continental crust.

The Kula volcanics show radiogenic Nd (ε_{Nd} as high as +6.3) and unradiogenic Sr isotopes (Figure 5A) although their Rb/Sr values show some variability (Figure 5B), possibly related to post-eruption mobilization of Rb. Our results are in agreement with previous isotopic measurements of Kula (Gulec 1991; Seyitoglu and Scott 1992; Alici et al. 2002). Nd isotopic compositions of these young lavas (as young as 0.025 million years, Richardson-Bunbury 1996) are, however, less radiogenic compared with those observed in young MORBs ($\varepsilon_{Nd} = +10$), which are derived from the depleted mantle and are distinctly different from arc lavas from Sunda, Banda, and the Lesser Antilles (Figure 5A). Primitive mantle-normalized trace element concentration patterns clearly rule out continental crustal contamination in these lavas due to lack of Nb–Ta anomaly, higher concentrations of Ba, etc. (Tatsumi and Eggins 1995). Based on the Nd–Sr isotopic composition and LREE enrichment of Kula, it might be suggested that these lavas are not derived from the depleted mantle but are low-degree partial melts of an OIB-like mantle. Pb isotopic composition of Kula overlaps with the composition of MORBs and OIBs (Figure 6A and 6B) and our results are consistent with those of Alici et al. (2002). The relatively unradiogenic Pb isotopic composition of the Kula lavas also suggests a major sub-lithospheric contribution.

In addition to the geochemical and isotopic compositions of the Kula lavas, which indicate their derivation from an OIB-like asthenospheric mantle, any model explaining the genesis of these volcanics has to take into account the role of extensional tectonics which was widespread during the eruption of these lavas. Lithospheric extension commonly produces melts from the asthenosphere upon decompression and this might well have been the mechanism by which the Kula lavas formed. In addition, lithosphere-scale extensional faults could have acted as natural conduits for the transport of these uncontaminated alkaline lavas (Figure 7).

Based on GPS studies, Doglioni *et al*. (2002) have proposed that the Aegean extension is due to differential convergence rates of the northeastward subducting African plate with respect to different parts of the Eurasian plate. Other workers (Tokcaer et al. 2005) considered the subducting African slab to be folded by the isostatic rebound of the mantle beneath the back-arc rift forming a horizontal slab window in the African plate that allowed asthenospheric upwelling. A slab-stretching scenario has also been proposed for the genesis of the Kula lavas (Innocenti et al. 2005). The association of the Kula volcanics within the Menderes massif is noteworthy and the uplift of this massif may have causal connection with the upwelling causing the Kula volcanics (Figure 1).

5. Overview of other geochemical and geophysical data

Given the available age relations, the major element concentrations of the volcanics studied here support the general contention that Cenozoic volcanism in Western Anatolia has evolved from an initial calc-alkaline magmatic episode, as seen in the comparatively older northern volcanics, to more mafic and alkali-rich phases over time, as observed in the rocks around Isparta and Kula volcanics. This compositional variation is also preserved in isotopes of fluid-mobile elements, for example Li (Agostini et al. 2008) and Pb (this study, Figure 6A and 6B), and is a result of the unique geodynamic setup of this region. Broadly, the sources of the volcanic products switch from supra-subduction orogenic suites to sub-slab asthenosphere (Innocenti et al. 2005). Lithospheric mantle contamination by older subduction-related fluids can generate calc-alkaline melts in a post-collisional setting (Sandvol et al. 2004). On the other hand, shoshonitic volcanism,

as documented in the Isparta region, is often associated with oblique convergence (Glover and Robertson 1998). Alkalic volcanism might also result from the interaction of a propagating back-arc rift with the volcanic arc, as documented in the Bonin–Mariana alkalic volcanic province (Wortel and Spakman 1992). Rifting may expose deeper and enriched portions of the mantle, which have not been melted previously.

Broad scale zones (~500 km) of low (<8 km/s) Pn velocities, often used to infer the rheology of the mantle, have been recorded below the Anatolian Plate suggesting the presence of hot and unstable mantle lid zones (McKenzie 1978), indicating the occurrence of widespread asthenosphere beneath Western Anatolia. Even lower Pn velocities (<7.8 km/s) beneath the IA indicate active asthenospheric upwelling in this region (McKenzie 1978). High heat flow in Western Anatolia is about 50% higher than the global average and reaches up to 300 mW/m^2, supporting active asthenospheric upwelling in this region (Pearce et al. 1990).

He isotopic ratio ($^3He/^4He$ with respect to atmospheric ratio, R/Ra) measurements in Turkey (0.05–7.87) (Gulec et al. 2002) are also important in this context. High $^3He/^4He$ indicates a dominantly mantle-derived He component in Central and Eastern Anatolia and in the Northern Anatolian Fault Zone (NAFZ) (Figure 1A and 1B); the NAFZ region also has a high geothermal potential. No He isotopic data are available from the Isparta region to the south. Although, the $^3He/^4He$ observed so far in geothermal fluids from Western Anatolia (0.2–3.6) (Gulec et al. 2002) does not clearly demonstrate the widespread existence of an asthenospheric source ($^3He/^4He = 8$) beneath this region; it is possible that the He isotopic composition of these geothermal fluids were affected by mixing with crustal fluids with much lower $^3He/^4He$. But, the radiogenic $\varepsilon_{Nd(0)}$ in the Western Anatolian volcanics of this study, as high as +6.4 to the north of the IAESZ and +6.3 for Kula, indicates the existence of shallow asthenosphere beneath Western Anatolia.

Much of Western and Central Anatolia used to be a highland marked by thickened continental crust (average ~40 km) and a high mean elevation (~3–4 km) in the aftermath of the Eocene collisional events in this region (Sengor et al. 1985). Seismic studies indicate a general trend of westward thinning of the crust from 36 km in Central Anatolia, to 28–30 km below the Central Menderes massif in Western Anatolia, to 25 km beneath the Aegean Sea (Bloomer et al. 1989). This westward thinning could possibly be due to regional extensional dynamics in this region.

GPS data indicate that the Western Anatolian Plate is rotating in a counterclockwise direction (Reilinger et al. 1997). Tectonic block rotations are often caused by transition from collision to normal subduction of a plate, which exerts a torque on the upper plate (Gurer et al. 2001). The rotation of the upper plate could also be facilitated by the presence of a low velocity zone close to the surface, as well as asthenospheric upwelling, for example in Kula and north of the IAESZ, as indicated by the isotopic and geochemical data presented above for Western Anatolia.

6. Chemical geodynamics of Western Anatolia

From the synthesis of other geochemical and geophysical data as well as our new data reported here, we have developed a chemical geodynamic model for Western Anatolia (Figure 7). The onset of post-collisional volcanism in Western Anatolia during the late Miocene and its evolution towards more alkaline compositions indicate important changes in thermal regimes, melt sources, and evolution patterns, as well as magma transport mechanisms beneath this region.

(1) The Samanli-Dag and Iznik–Mudanya volcanic rocks to the north of the IAESZ were formed in a subduction zone setting, as reflected in their major and trace element compositions induced by partial melting of the metasomatized Neotethyan mantle-wedge. Given that these post-collisional volcanic rocks were not formed during active subduction, partial melting of the subduction-metasomatized Neotethyan mantle-wedge was aided by heat derived from asthenospheric upwelling, resulting from the delamination of the subducting Neotethyan slab. Radiogenic Nd isotopic compositions of these volcanic rocks ($\varepsilon_{Nd(0)}$ as high as +6.4), in particular, indicate widespread upwelling asthenosphere beneath this region and rule out their derivation from a lithospheric mantle source.

(2) The calc-alkaline Bigadic–Sindirgi and alkaline Seyitgazi volcanic rocks, located within the IAESZ, show the clear imprint of subduction-related fluids in their trace element and enriched Nd–Sr isotopic compositions, whereas their high $^{207}Pb/^{204}Pb$, similar to the Sunda arc lavas, indicates assimilation of ancient crustal rocks. There is also clear geochemical indication of the involvement of the continental lithospheric mantle. These post-collisional volcanic rocks were formed by partial melting of the lithospheric mantle during extensional tectonics; the latter was metasomatized by fluids from an earlier episode of subduction of the Neotethyan slab. The Simav–Usak volcanics, hosted in the Menderes massif, were similarly formed.

(3) The Kirka, Afyon–Suhut, Golcuk–Isparta, and Senirkent volcanic rocks located along the N–S-oriented KAI structural trend show the clear imprint of subduction-related fluids in their trace element compositions, similar to the Simav–Usak

volcanic rocks, which lie off this trend. The Golcuk–Isparta volcanic rocks are compositionally distinct from the other volcanic rocks along the KAI trend in having very high trace element concentrations, fractionated LREE, relatively depleted Nd–Sr isotopes, and very low Rb/Sr. Their Pb isotopic compositions are unique and are similar to those of MORB. Based on these new data, we propose a chemical geodynamic model in which the lithospheric mantle sources of the alkaline volcanic rocks along the KAI structural trend as well as the Afyon–Suhut volcanic rocks were metasomatized by fluids from an older episode of subduction. The Golcuk–Isparta volcanic rocks were derived from an asthenospheric source. Asthenospheric upwelling resulted from a tear in the subducting African lithosphere due to differences in subducting plate velocities along the Hellenic and Cyprean trenches.

(4) The alkaline Kula volcanic rocks are unique in their geochemical and isotopic compositions: these include $\varepsilon_{Nd(0)}$ as high as +6.3 and enriched trace element patterns including lack of negative Nb–Ta anomalies (Figure 3B), indicating their derivation from an OIB-like asthenospheric mantle source. These young volcanic rocks were erupted when regional extensional tectonics was widespread and lithosphere-scale extensional faults could have acted as natural conduits for the transport of these uncontaminated alkaline lavas. Decompressional melting of the asthenospheric source resulting from lithospheric extension can explain the origin of the Kula volcanic rocks. Alternatively, a horizontal slab window in the subducting African slab, resulting from different velocities of the Greek and Anatolian microplates with respect to a fixed African plate, could also have allowed asthenospheric upwelling in the Kula region.

(5) Radiogenic Nd isotopic compositions of the post-collisional volcanic rocks from Western Anatolia, both north and south of the IAESZ, suggest the presence of shallow asthenosphere beneath Anatolia. This conclusion is in agreement with low Pn wave velocities observed in Western Anatolia. Rising asthenosphere beneath this region could explain the observed high seismicity, tectonic activity, and measured rapid rotation of the Anatolian Plate.

Acknowledgements

The geochemical aspect of this study was supported by NSF grants to ARB. The samples for this study were provided by Y. Dilek and S. Altunkaynak.

References

Agostini, S., Ryan, J.G., Tonarini, S., and Innocenti, F., 2008, Drying and dying of a subducted slab: Coupled Li and B isotope variations in Western Anatolia Cenozoic Volcanism: Earth and Planetary Science Letters, v. 272, p. 139–147.

Akay, E., and Erdogan, B., 2004, Evolution of Neogene calc-alkaline to alkaline volcanism in the Aliaga-Foca region (Western Anatolia, Turkey): Journal of Asian Earth Sciences, v. 24, p. 367–387.

Aldanmaz, E., Koprubasi, N., Gurer, O.F., Kaymakci, N., and Gourgaud, A., 2006, Geochemical constraints on the Cenozoic, OIB-type alkaline volcanic rocks of NW Turkey: Implications for mantle sources and melting processes: Lithos, v. 86, p. 50–76.

Aldanmaz, E., Pearce, J.A., Thirlwall, M.F., and Mitchell, J.G., 2000, Petrogenetic evolution of late Cenozoic, post-collision volcanism in western Anatolia, Turkey: Journal of Volcanology and Geothermal Research, v. 102, p. 67–95.

Alici, P., Temel, A., and Gourgaud, A., 2002, Pb-Nd-Sr isotope and trace element geochemistry of Quaternary extension related alkaline volcanism: A case study of Kula region (western Anatolia, Turkey: Journal of Volcanology and Geothermal Research, v. 115, p. 487–510.

Al-Lazki, A.I., Sandvol, E., Seber, D., Barazangi, M., Turkelli, N., and Mohamad, R., 2004, Pn tomographic imaging of mantle lid velocity and anisotropy at the junction of the Arabian, Eurasian and African plates: Geophysical Journal International, v. 158, p. 1024–1040.

Altunkaynak, S., 2007, Collision-drived slab breakoff magmatism in Northwestern Anatolia, Turkey: The Journal of Geology, v. 115, p. 63–82.

Altunkaynak, S., and Genc, S.C., 2008, Petrogenesis and time-progressive evolution of the Cenozoic continental volcanism in the Biga Peninsula, NW Anatolia (Turkey): Lithos, v. 102, p. 316–340.

Barka, A., Reilinger, R.E., Saroglu, F., and Sengor, A.M.C., 1997, The Isparta Angle: Its evolution and importance in the tectonics of the eastern Mediterranean region: International Earth Sciences Colloquium on Aegean region – IESCA95, v. 1, p. 3–17.

Basu, A.R., Sharma, M., and DeCelles, P.G., 1990, Nd, Sr-isotopic provenance and trace element geochemistry of Amazonian foreland basin fluvial sands, Bolivia and Peru: Implications for ensialic Andean Orogeny: Earth and Planetary Science Letters, v. 100, p. 1–17.

Bloomer, S.H., Stern, R.J., Fisk, E., and Geschwind, C.H., 1989, Shoshonitic volcanism in the northern Mariana arc – Mineralogic and major and trace element characteristics: Journal of Geophysical Research, v. 94, p. 4469–4496.

Bozkurt, E., 2001, Neotectonics of Turkey – A synthesis: Geodinamica Acta, v. 14, p. 3–30.

Bozkurt, E., 2003, Origin of NE-trending basins in western Turkey: Geodinamica Acta, v. 16, p. 61–81.

Bozkurt, E., and Park, R.G., 1994, Southern Menderes Massif: An incipient metamorphic core complex in western Anatolia, Turkey: Journal of the Geological Society, London, v. 151, p. 213–216.

Candan, O., Cetinkaplan, M., Oberhansli, R., Rimmele, G., and Akal, C., 2005, Alpine high-P/low-T metamorphism of the Afyon zone and implications for the metamorphic evolution of Western Anatolia: Lithos, v. 84, p. 102–124.

Catlos, E.J., and Cemen, I., 2005, Monazite ages and the evolution of the Menderes Massif, western Turkey: International Journal of Earth Sciences (Geologische Rundschau), v. 94, p. 204–217.

Çoban, H., and Flower, M.F.J., 2007, Late Pliocene lamproites from Bucak, Isparta (southwestern Turkey): Implications for mantle 'wedge' evolution during Africa-Anatolian Plate convergence: Journal of Asian Earth Sciences, v. 29, p. 160–176.

Cole, R.B., and Basu, A.R., 1992, Middle Tertiary volcanism during ridge-trench interactions in western California: Science, v. 258, p. 793–796.

Coulon, C., Megartsi, M., Fourcade, S., Maury, R.C., Bellon, H., Louni-Hacini, A., Cotten, J., Coutelle, A., and Hermitte, D., 2002, Post-collisional transition from calc-alkaline to alkaline volcanism during the Neogene in Oranie (Algeria): Magmatic expression of a slab breakoff: Lithos, v. 62, p. 87–110.

Davis, J., and Hawkesworth, C.J., 1993, Petrogenesis of 30–20 Ma basic and intermediate volcanics from the Mogollon-Datil volcanic field, New Mexico, USA: Contributions to Mineralogy and Petrology, v. 115, p. 165–183.

DePaolo, D.J., 1988, Neodymium isotope geochemistry, *in* Minerals and rocks: Heidelberg, Springer Verlag, p. 187.

Dilek, Y., and Altunkaynak, S., 2007, Cenozoic crustal evolution and mantle dynamics of post-collisional magmatism in western Anatolia: International Geology Review, v. 49, p. 431–453.

Dilek, Y., and Moores, E.M., 1990, Regional tectonics of the eastern Mediterranean ophiolites, *in* Malpas, J., and Moores, E.M., eds., Ophiolites; oceanic crustal analogues; Proceedings of the symposium "Troodos 1987": Nicosia, Cyprus, Geological Survey Department, p. 295–309.

Doglioni, C., Agostini, S., Crespi, M., Innocenti, F., Menetti, P., Riguzzi, F., and Savascin, Y., 2002, On the extension in western Anatolia and the Aegean sea: Journal of the Virtual Explorer, v. 8, p. 169–183.

Ercan, T., Satir, M., Steinitz, G., Dora, A., Sarifakioglu, E., Adis, C., Walter, H.J., and Yildrim, T., 1995, Characteristics of the Tertiary volcanism in the Biga Peninsula, Gokceada, Bozcaada and Tavsanadasi, NW Anatolia: Bulletin Geological Society of Turkey, v. 28, p. 121–136.

Erkul, F., Helvaci, C., and Sozbilir, H., 2005, Evidence for two episodes of volcanism in the Bigadic, borate basin and tectonic implications for western Turkey: Geological Journal, v. 40, p. 545–570.

Ersoy, Y., and Helvaci, C., 2007, Stratigraphy and geochemical features of the early Miocene bimodal (Ultrapotassic and Calc-alkaline) volcanic activity within the NE-trending Selendi basin, Western Anatolia, Turkey: Turkish Journal of Earth Sciences, v. 16, p. 117–139.

Ersoy, Y., Helvaci, C., Sozbilir, H., Erkul, F., and Bozkurt, E., 2008, A geochemical approach to Neogene-Quaternary volcanic activity of western Anatolia: An example of episodic bimodal volcanism within the Selendi Basin, Turkey: Chemical Geology, v. 255, p. 265–282.

Faccenna, C., Bellier, O., Martinod, J., Piromallo, C., and Regard, V., 2006, Slab detachment beneath eastern Anatolia: A possible cause for the formation of the Northern Anatolian fault: Earth and Planetary Science Letters, v. 242, p. 85–97.

Glover, C., and Robertson, A., 1998, Neotectonic intersection of the Aegean and Cyprus tectonic arcs: Extensional and strike-slip faulting in the Isparta Angle, SW Turkey: Tectonophysics,v. 298, p. 103–132.

Gulec, N., 1991, Crust-mantle interaction in western Turkey: Implications from Sr and Nd isotope geochemistry of Tertiary and Quaternary volcanics: Geological Magazine, v. 128, p. 417–435.

Gulec, N., Hilton, D.R., and Mutlu, H., 2002, Helium isotopic variations in Turkey: Relationship to tectonics, volcanism and recent seismic activities: Chemical Geology, v. 187, p. 129–142.

Gurer, A., Bayrak, M., and Gurer, O.F., 2004, Magnetotelluric images of crust and mantle in the southwestern Taurides, Turkey: Tectonophysics, v. 391, p. 109–120.

Gurer, A., Gurer, O.F., Pince, A., and Ilkisik, O.M., 2001, Conductivity structure along the Gediz graben, west Anatolia, Turkey: Tectonic implications: International Geology Review, v. 43,p. 1129–1144.

Harris, N.B.W., Kelley, S., and Okay, A.I., 1994, Post-collision magmatism and tectonics in Northwest Anatolia: Contributions to Mineralogy and Petrology, v. 117, p. 241–252.

Hawkesworth, C.J., 1979, $^{143}Nd/^{144}Nd$, $^{87}Sr/^{86}Sr$ and trace element characteristics of magmas along destructive plate margins, *in* Atherton, M.P., and Tarney, J., eds., Origin of granite batholiths: UK, Shiva Publishing Ltd., p. 76–89.

Hawkesworth, C.J., Norry, M.J., Roddick, J.C., Baker, P.E., Francis, P.W., and Thorpe, R.S., 1979a, $^{143}Nd/^{144}Nd$, $^{87}Sr/^{86}Sr$, and incompatible element variations in calc-alkaline andesites and plateau lavas from South America: Earth and Planetary Science Letters, v. 42, p. 45–57.

Hawkesworth, C.J., O'Nions, R.K., and Arculus, R.J., 1979b, Nd and Sr isotope geochemistry of island arc volcanics, Grenada, Lesser Antilles: Earth and Planetary Science Letters, v. 45,p. 237–248.

Hawkesworth, C.J., and Powell, M., 1980, Magma genesis in the Lesser Antilles island arc: Earth and Planetary Science Letters, v. 51, p. 297–308.

Hegner, E., and Smith, I.E.M., 1992, Isotopic compositions of late Cenozoic volcanics from Papua New Guinea: Evidence for multi-component sources in arc and rift environments: Chemical Geology, v. 97, p. 233–249.

Hofmann, A.W., Jochum, K.P., Seufer, M., and White, W.M., 1986, Nb and Pb in oceanic basalts: New constraints on mantle evolution: Earth and Planetary Science Letters, v. 79, p. 33–45.

Houseman, G.A., McKenzie, D.P., and Molnar, P., 1981, Convective instability of a thickened boundary layer and its relevance for the thermal evolution of continental convergent belts: Journal of Geophysical Research, v. 86, p. 6115–6132.

Innocenti, F., Agostini, S., Di Vincenzo, G., Doglioni, C., Manetti, P., Savascin, M.Y., and Tonarini, S., 2005, Neogene and Quaternary volcanism in Western Anatolia: Magma sources and geodynamic evolution: Marine Geology, v. 221, p. 397–421.

Innocenti, F., Manetti, P., Mazzuoli, R., Pasquare, G., and Villari, L., 1982, Anatolia and northwestern Iran, *in* Thorpe, R.S., ed., Andesites: Orogenic andesites and related rocks: New York, JohnWiley and Sons, p. 327–349

Jackson, J., and McKenzie, D., 1988a, Rates of active deformation in the Aegean Sea and surrounding areas: Basin Research, v. 1, p. 121–128.

Jackson, J., and McKenzie, D., 1988b, The relationship between plate motions and seismic moment tensors, and the rates of active deformation in the Mediterranean and Middle East: Geophysical Journal of the Royal Astronomical Society, v. 93, p. 45–73.

Jolivet, L., Daniel, J.M., Truffert, C., and Goffé, B., 1994, Exhumation of deep crustal metamorphic rocks and crustal extension in arc and back-arc regions: Lithos, v. 33, p. 3–30.

Kocyigit, A., and Ozacar, A., 2003, Extensional neotectonic regime through the NE edge of the outer Isparta Angle, SW Turkey: New field and seismic data: Turkish Journal of Earth Sciences, v. 12, p. 67–90.

Koprubasi, N., and Aldanmaz, E., 2004, Geochemical constraints on the petrogenesis of Cenozoic I-type granitoids in

Northwest Anatolia, Turkey: Evidence for magma generation by lithospheric delamination in a post-collisional setting: International Geology Review, v. 46, p. 705–729.

Le Bas, M.J., and Streckeisen, A.L., 1991, The IUGS systematics of igneous rocks: Journal of the Geological Society, London, v. 148, p. 825–833.

Le Pichon, X., Chamot-Rooke, N., Lallemant, S., Noomen, R., and Veisothers, G., 1995, Geodetic determination of the kinematics of central Greece with respect to Europe: Implications for eastern Mediterranean tectonics: Journal of Geophysical Research, v. 100, p. 12675–12690.

McClusky, S., and Balassanian, S., 2000, Global positioning system constraints on plate kinematics and dynamics in the eastern Mediterranean and Caucasus: Journal of Geophysical Research,v. 105, p. 5695–5719.

McKenzie, D., 1972, Active tectonics in the Mediterranean region: Geophysical Journal Royal Astronomical Society, v. 30, p. 109–185.

McKenzie, D., 1978, Active tectonics of the Alpine-Himalayan belt: The Aegean sea and surrounding regions: Geophysical Journal of the Royal Astronomical Society, v. 55, p. 217–254.

Meulenkamp, J.E., Wortel, M.J.R., van Wamel, W.A., Spakman, W., and Hoogerduyn Strating, E., 1988, On the Hellenic subduction zone and the geodynamic evolution of Crete since the late middle Miocene: Tectonophysics, v. 146, p. 203–215.

Miller, D.M., Goldstein, S.L., and Langmuir, C.H., 1994, Cerium/lead and lead isotope ratios in arc magmas and the enrichment of lead in the continents: Nature, v. 368, p. 514–520.

Okay, A.I., Harris, N.B.W., and Kelley, S.P., 1998, Exhumation of blueschists along a Tethyan suture in Northwest Turkey: Tectonophysics, v. 285, p. 275–299.

Okay, A.I., and Satir, M., 2000, Coeval plutonism and metamorphism in a latest Oligocene metamorphic core complex in northwest Turkey: Geological Magazine, v. 137, p. 495–516.

Okay, A.I., and Satir, M., 2002, When and why did the extension start in the Aegean? Geological Society of America Annual Meeting, Denver, CO, Abstracts with Programs, v. 34, no. 6, p. 179.

Onions, R.K., Hamilton, P.J., and Evensen, N.M., 1977, Variations in Nd-143/Nd-144 and Sr-87/Sr-86 Ratios in Oceanic Basalts: Earth and Planetary Science Letters, v. 34, p. 13–22.

Oral, M.B., Reilinger, R.E., Toksoz, M.N., King, R.W., Barka, A.A., and Kinik, I., 1995, Global Positioning System offers evidence of plate motions in eastern Mediterranean: Eos, Transactions, American Geophysical Union, v. 76, p. 9–11.

Pearce, J.A., 1983. Role of the subcontinental lithosphere in magma genesis at active continental margins, *in* Hawkesworth, C.J., and Norry, M.J., eds., Continental basalts and mantle xenoliths: Nantwich, U.K., Shiva Publication, p. 230–249.

Pearce, J.A., Bender, J.F., DeLong, S.E., Kidd, W.S.F., Low, P.J., Guner, Y., Saroglu, F., Yilmaz, Y., Moorbath, S., and Mitchell, J.G., 1990, Genesis of collision volcanism in Eastern Anatolia, Turkey: Journal of Volcanology and Geothermal Research, v. 44, p. 189–229.

Peccerillo, A., and Taylor, S.R., 1976, Geochemistry of Eocene calc-alkaline volcanic rocks from the Kastamonu area, Northern Turkey: Contributions to Mineralogy and Petrology, v. 58, p. 63–81.

Pe-Piper, G., and Piper, D.J.W., 2001, Late Cenozoic, post-collisional Aegean igneous rocks: Nd, Pb and Sr isotopic constraints on petrogenetic and tectonic models: Geological Magazine, v. 138,p. 653–668.

Piper, J.D.A., Gursoy, H., Tatar, O., Isseven, T., and Kocyigit, A., 2002, Paleomagnetic evidence for the Gondwanian origin of the Taurides and rotation of the Isparta Angle, southern Turkey: Geological Journal, v. 37, p. 317–336.

Plank, T., 2005, Constraints from thorium/lanthanum on sediment recycling at subduction zones and the evolution of the continents: Journal of Petrology, v. 46, p. 921–944.

Reilinger, R.E., McClusky, S.C., and Oral, M.B., 1997, Global Positioning System measurements of present-day crustal movements in the Arabia-Africa-Eurasia plate collision zone: Journal of Geophysical Research, v. 102, p. 9983–9999.

Richardson-Bunbury, J.M., 1996, The Kula volcanic field, western Turkey: The development of a Holocene alkali basalt province and the adjacent normal faulting graben: Geological Magazine, v. 133, p. 275–283.

Rollinson, H., 1993, Using geochemical data: Evaluation, presentation and interpretation: London, Longman Scientific and Technical, p. 352.

Salters, V.J.M., and Hart, S.R., 1991, The mantle sources of ocean ridges, islands and arcs: The Hf-isotope connection: Earth and Planetary Science Letters, v. 104, p. 364–380.

Sandvol, E., Gomez, F., and Cemen, I., 2004, Mantle dynamics and continental deformation resulting from slab-tear beneath the Isparta-Angle in southwestern Turkey: Geological Society of America Annual Meeting, Denver, CO, v. 36, no 5, p. 5.

Savascin, M.Y., 1990, Magmatic activities of Cenozoic compressional and extensional regimes in western Anatolia: International Earth Science Congress Aegean Regions, Izmir, Turkey, v., p. 420–434.

Savascin, M.Y., and Oyman, T., 1998, Tectono-magmatic evolution of alkaline volcanics at the Kirka-Afyon-Isparta structural trend, SW Turkey: Turkish Journal of Earth Sciences, v. 7, p. 201–214.

Sengor, A.M.C., Gorur, N., and Saroglu, F., 1985, Strike-slip deformation and related basin formation in zones of tectonic escape – Turkey as a case study: Society of Economic Paleontologists and Mineralogist Special Publication, v. 37, p. 227–264.

Sengor, A.M.C., and Yilmaz, Y., 1981, Tethyan evolution of Turkey: A plate tectonic approach: Tectonophysics, v. 75, p. 181–241.

Seyitoglu, G., Anderson, D., Nowell, G., and Scott, B., 1997, The evolution from Miocene potassic to Quaternary sodic magmatism in western Turkey: Implications for enrichment processes in the lithospheric mantle: Journal of Volcanology and Geothermal Research, 76, p. 127–147.

Seyitoglu, G., and Scott, B.C., 1992, Late Cenozoic volcanic evolution of the NE Aegean region: Journal of Volcanology and Geothermal Research, v. 54, p. 157–176.

Seyitoglu, G., and Scott, B.C., 1996, The cause of N-S extensional tectonics in Western Turkey: Tectonic escape vs back-arc spreading vs orogenic collapse: Journal of Geodynamics, v. 22, p. 145–153.

Sharma, M., Basu, A.R., and Nesterenko, G.V., 1992, Temporal Sr, Nd and Pb isotopic variations in the Siberian flood basalts: Implications for the plume-source characteristics Earth and Planetary Science Letters, v. 113, p. 365–381.

Sun, S.-S., and McDonough, W.F., 1989, Chemical and isotopic systematics of oceanic basalts: Implications for mantle composition and processes, *in* Saunders, A.D., and Norry, M.J., eds., Magmatism in the ocean basins: Geological Society of London Special Publication 42, p. 315–345.

Tatsumi, Y., and Eggins, S., 1995, Subduction zone magmatism, *in* Hofmann, A.W., Jeanloz, R., and Knoll, A.H., eds., Frontiers in earth sciences: Cambridge, MA, Blackwell Science, p. 211.

Taylor, R.N., and Nesbitt, R.W., 1998, Isotopic characteristics of subduction fluids in an intra-oceanic setting, Izu-Bonin Arc, Japan: Earth and Planetary Science Letters, v. 164, p. 79–98.

Taymaz, T., Jackson, J., and McKenzie, D., 1991, Active tectonics of the central Aegean Sea: Geophysical Journal International, v. 106, p. 433–490.

Tekeli, O., 1981, Subduction complex of pre-Jurassic age, Northern Anatolia: Geology, v. 9, p. 68–72.

Tokcaer, M., Agostini, S., and Savascin, M.Y., 2005, Geotectonic setting and origin of the youngest Kula volcanics (Western Anatolia), with a new emplacement model: Turkish Journal of Earth Sciences, v. 14, p. 145–166.

Venturelli, G., Thorpe, R.S., Dal Piaz, G.V., Del Moro, A., and Pohs, P.J., 1984, Petrogenesis of calc-alkaline, shoshonitic and associated ultrapotassic Oligocene volcanic rocks from the northwestern Alps, Italy: Contributions to Mineralogy and Petrology, v. 86, p. 209–220.

Whitford, D.J., White, W.M., and Jezek, P.A., 1981, Neodymium isotopic composition of Quaternary island arc lavas from Indonesia: Geochimica et Cosmochimica Acta, v. 45, p. 989–995.

Wortel, M.J.R., and Spakman, W., 1992, Structure and dynamics of subducted lithosphere in the Mediterranean region: Proceedings of the Koninklijke Nederlandse Akademie van Wetenschappen, v. 9, p. 32–347.

Yagmurlu, F., Savascin, M.Y., and Ergun, M., 1997, Relation of the alkaline volcanism and active tectonism within the evolution of Isparta Angle, SW Turkey: Journal of Geology, v. 105, p. 23.

Yılmaz, K., 2010, Origin of anorogenic 'lamproite-like' potassic lavas from the Denizli region in Western Anatolia Extensional Province, Turkey: Mineralogy and Petrology, v. 99, p. 219–239.

Yilmaz, Y., 1989, An approach to the origin of young volcanic rocks of western Turkey, *in* Sengor, A.M.C., ed., Tectonic evolution of the Tethyan region: Dordrecht, Kluwer Academic Publishers, p. 159–189.

Yilmaz, Y., 1990, Comparison of young volcanic associations of western and eastern Anatolia formed under a compressional regime: A review: Journal of Volcanology and Geothermal Research, v. 44, p. 69–87.

Yilmaz, Y., Genc, S.C., Karacik, Z., and Altunkaynak, S., 2001, Two contrasting magmatic associations of NW Anatolia and their tectonic significance: Journal of Geodynamics, v. 31, p. 243–271.

Appendix 1. Analytical methods

Whole-rock sample chips showing no surficial alteration were hand picked, were sonicated for 30 minutes in deionized water, and were powdered in an alumina spex ball mill. Major elements were analysed in a commercial laboratory, Actlabs (Ontario, Canada). The samples underwent lithium metaborate/tetraborate fusion followed by measurement using an ICP-OES (inductively coupled plasma optical emission spectrometry). Repeated measurements of known rock standards indicate that the concentrations of the major elements are within 0.2% and are also certified as such by the laboratory. Reported major element data have not been normalized to 100.

Trace element concentrations were measured using an inductively coupled plasma mass spectrometer (ICPMS, Thermo elemental X-7 series) at the University of Rochester. For ICPMS analyses in our laboratory, 25 mg of powdered rock samples were digested in HF–HNO_3 acid mixtures and diluted to 100 ml of 2% HNO_3 solution with ~10 ppb In, Cs, Re, and Bi internal standard. The elemental concentrations of the samples were obtained by using BCR-2 and BIR-2 (basalts, concentrations from USGS) as known external standards. The concentrations of the various elements are within 5% error, commonly at 2% for the REEs, as estimated from repeated measurements of AGV-2 (andesite-USGS) and BHVO-2 (basalt-USGS) rock standards that were run as unknowns.

For isotopic analyses, 100–200 mg of powdered samples was dissolved in HF–HNO_3 and HCl acids. Nd-, Sr-, and Pb isotopic ratios were measured with a thermal ionization mass spectrometer (TIMS, VG Sector) using the procedures established for our laboratory at the University of Rochester (Basu et al. 1990). Measured $^{87}Sr/^{86}Sr$ ratios were normalized to $^{86}Sr/^{88}Sr = 0.1194$. Uncertainties for the measured $^{87}Sr/^{86}Sr$ were less than 4 in the fifth decimal place. The NBS-987 Sr standard analysed during the course of this study yielded $^{87}Sr/^{86}Sr = 0.710245 \pm 0.000023$ (2σ) ($n = 5$). Selected rock samples showing comparatively radiogenic Sr isotopic compositions (see discussion) were reanalysed to investigate the possibility of post-magmatic alteration. Rock chips of these samples were sonicated in dilute HCl acid and washed with deionized water before crushing and acid digestion. Sr isotopic compositions of the acid-leached samples are identical to the unleached fractions of the same samples and are hence not reported separately. Measured $^{143}Nd/^{144}Nd$ ratios were normalized to $^{146}Nd/^{144}Nd = 0.7219$ (Onions et al. 1977). Uncertainties for the measured $^{143}Nd/^{144}Nd$ ratios were less than 3 in the fifth decimal place. La Jolla Nd standard analysed during the course of this study yielded $^{143}Nd/^{144}Nd = 0.511852 \pm 24$ (2σ) ($n = 6$) where the errors correspond to the last two digits. Pb isotopes were measured using the silica-gel technique by TIMS, also at the University of Rochester (Sharma et al. 1992). Filament temperature during Pb isotope ratio measurements was monitored continuously and raw ratios were calculated as weighted averages of the ratios measured at 1150°C, 1200°C, and 1250°C. The reported Pb isotopic data are corrected for mass fractionation of $0.12 \pm 0.03\%$ per amu based on replicate analyses of the NBS-981 Equal Atom Pb standard measured in the same fashion. Our laboratory procedural blanks were less than 400 pg for Sr and less than 200 pg for both Nd and Pb. No blank correction was necessary for the isotope ratios measured.